A chemical model for the atmosphere of hot Jupiters

O. Venot[1,2], E. Hébrard[1,2], M. Agúndez[1,2], M. Dobrijevic[1,2], F. Selsis[1,2], F. Hersant[1,2], N. Iro[3,4], and R. Bounaceur[5]

[1] Univ. Bordeaux, LAB, UMR 5804, F-33270, Floirac, France
e-mail: `venot@obs.u-bordeaux1.fr`
[2] CNRS, LAB, UMR 5804, F-33270, Floirac, France
[3] Astrophysics Group, Keele University, Keele, Staffordshire, ST5 5BG, UK
[4] LESIA, Observatoire de Paris, 5 Place Jules Janssen, F-92195 Meudon, France
[5] Laboratoire Réactions et Génie des Procédés, LRGP UPR 3349 CNRS, Université de Lorraine, 1 rue Grandville, BP 20401, F-54001 Nancy, France

ABSTRACT

Context. The atmosphere of hot Jupiters can be probed by primary transit and secondary eclipse spectroscopy. Due to the intense UV irradiation, mixing and circulation, their chemical composition is maintained out of equilibrium and must be modeled with kinetic models.

Aims. Our purpose is to release a chemical network, and the associated rate coefficients, developed for the temperature and pressure range relevant to hot Jupiters atmospheres. Using this network, we study the vertical atmospheric composition of the two hot Jupiters (HD 209458b and HD 189733b) with a model that includes photolyses and vertical mixing and we produce synthetic spectra.

Methods. The chemical scheme is derived from applied combustion models that have been methodically validated over a range of temperatures and pressures typical of the atmospheric layers influencing the observations of hot Jupiters. We compare the predictions obtained from this scheme with equilibrium calculations, with different schemes available in the literature that contain N-bearing species and with previously published photochemical models.

Results. Compared to other chemical schemes that were not subjected to the same systematic validation, we find significant differences whenever non-equilibrium processes take place (photodissociations or vertical mixing). The deviations from the equilibrium, and thus the sensitivity to the network, are more important for HD 189733b, as we assume a cooler atmosphere than for HD 209458b. We found that the abundances of NH_3 and HCN can vary by two orders of magnitude depending on the network, demonstrating the importance of comprehensive experimental validation. A spectral feature of NH_3 at 10.5 μm is sensitive to these abundance variations and thus to the chemical scheme.

Conclusions. Due to the influence of the kinetics, we recommend the use of a validated scheme to model the chemistry of exoplanet atmospheres. The network we release is robust for temperatures within 300-2500 K and pressures from 10 mbar up to a few hundreds of bars, for species made of C, H, O, N. It is validated for species up to 2 carbon atoms and for the main nitrogen species (NH_3, HCN, N_2, NO_X). Although the influence of the kinetic scheme on the hot Jupiters spectra remains within the current observational error bars (with the exception of NH_3), it will become more important for atmospheres that are cooler or subjected to higher UV fluxes, departing more from equilibrium.

Key words. Astrochemistry – Planets and satellites: atmospheres – Planets and satellites: individual: (HD 209458b - HD 189733b)

1. Introduction

So far, more than 700 exoplanets have been confirmed and thousands of transiting candidates have been identified by the space telescope Kepler (Batalha et al. 2012). Among them, hot Jupiters are a class of gas giants with orbital periods of a few days or less. They are found around ∼ 0.5% of KGF stars (Howard et al. 2010, 2012). About 10% of them transit their host star and their atmospheric composition and physical structure can be studied by transit spectroscopy (e.g. Charbonneau et al. 2000, 2008; Richardson et al. 2007; Tinetti et al. 2007; Sing et al. 2008; Swain et al. 2008a,b, 2009a,b; Huitson et al. 2012).

Although current observations are still limited and subjected to divergent interpretations, future instruments such as E-ELT, JWST (Gardner et al. 2006), EChO (Tinetti et al. 2011), FINESSE (Swain 2010) should provide better constraints on both the chemical composition and the temperature profiles of the nearby hot Jupiters like HD 189733b and HD 209458b. They

will also be able to study more distant targets and deliver statistically significant trends about the nature of their atmospheres. Chemical modeling will be an important component of these studies. It will point to key observations able to distinguish between various hypotheses and will be used to analyze the observations and constrain, for instance, the atmospheric elemental abundances.

The first models of hot Jupiter atmospheres assumed chemical equilibrium (e.g. Burrows & Sharp 1999; Seager & Sasselov 2000; Sharp & Burrows 2007; Barman 2007; Burrows et al. 2007, 2008; Fortney et al. 2008a). However, strongly irradiated atmospheres are unlikely to be at chemical equilibrium. Their intense UV irradiation (typically 10,000 times the flux received on the top of the atmosphere of Jupiter) and strong dynamics result in photolyses and diffusion/advection timescales that are comparable or shorter than the chemical ones. Deviations from the thermodynamic equilibrium have been discussed with timescale arguments (e.g. Lodders & Fegley

2002; Fortney et al. 2006, 2008b; Visscher et al. 2006, 2010; Madhusudhan & Seager 2010), or modeled with a few reactions describing the CO-CH$_4$ conversion coupled with the dynamics (Cooper & Showman 2006). A more detailed modeling requires the use of a photochemical kinetic network. A kinetic network is, in practice, a list of reactions and associated rate coefficients able to describe quantitatively (within a certain accuracy) the kinetics of a pool of species, usually the most abundant ones. Constructing such network of reactions implies to solve two major questions. One has to do with the completeness of the network: What are the species and the reactions connecting them that must be included? The other issue is the availability of the kinetic data: The literature and databases may not provide the rate coefficients for some of the needed reactions or may provide conflicting values with no recommendation. These two issues are tightly connected and both depend on the considered range of temperatures and pressures. Eventually, and whatever the methodology adopted to select the reactions and their rates, it is the ability to predict experimentaly-controled abundances that can validate or not the network.

To investigate the consequences of the strong UV incident flux on neutral species, photochemical models have then been developed (Liang et al. 2003, 2004). Based on kinetics model dedicated to Jupiter's low-temperature atmosphere, these models however neglected endothermic reactions, which are in fact rather efficient in such hot atmospheres. Line et al. (2010) introduced some endothermic reactions to a similar Jovian photochemical scheme but most of the pre-existing reactions were not reversed. They were therefore not able to reproduce the thermodynamic equilibrium, which occurs in the deep atmospheres of hot Jupiters. Zahnle et al. (2009a,b) developed a photochemical model considering the reversal of their whole set of two-bodies exothermic reactions. They selected their rate constants in the NIST database[1] based on the following criteria: relevance of temperature conditions, date of review, date of the experiment and date of the theoretical study (in order of preference). Moses et al. (2011) developed a model that considered the reversal of all the reactions, including three-body reactions, ensuring to reproduce the thermodynamical equilibrium from the top to the deepest layers of the atmosphere. Their chemical scheme is derived from the Jupiter and Saturn models (Gladstone et al. 1996; Moses 1996; Moses et al. 1995b,a, 2000a,b) with further updates on the basis of combustion-chemistry literature. None of the aforementioned works discuss the validation of the chemical scheme against experiments. In addition, the fact that computed abundances evolve towards the composition predicted by equilibrium calculations (at given pressure P and temperature T with no external irradiation nor mixing) is by no means a validation of the kinetic network. Indeed, any network containing at least as many independent reversible reactions as modeled species, in which the rates for the backward processes are derived from equilibrium constants and forward rates, will evolve toward the equilibrium predicted with the same equilibrium constants, whatever the quantitative values of the forward rates, as illustrated in Fig. 1. Fortunately, and due to the physical conditions and elemental composition of hot Jupiters (and hot Neptunes) atmospheres, we benefit from decades of intensive work done in the field of combustion, that includes a vast amount of experiments, the development of comprehensive mechanisms[2] and the
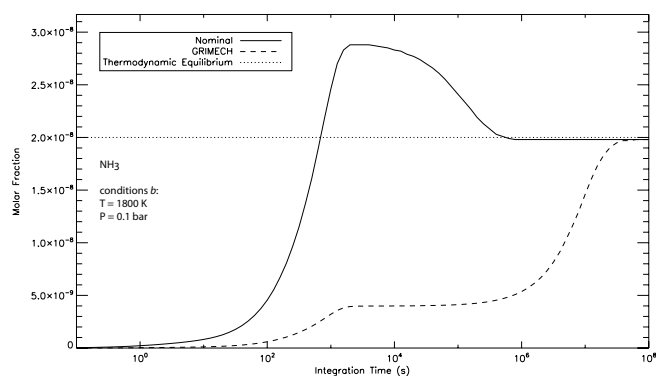

Fig. 1: Abundances of NH$_3$ as a function of time computed with two kinetic schemes fully reversed according to equilibrium constants but differing by their nitrogen chemistry (nominal and *GRIMECH* as defined in Sects. 2.1.2 and 3.3). While they both converge towards the equilibrium (dotted line) they exhibit very different evolution. Initial condition is a mixture of H$_2$, CH$_4$, O$_2$, N$_2$ and He with solar elemental abundances.

systematic comparison between the two. Therefore, we propose in the present work a new mechanism dedicated to the chemical modeling of hot atmospheres that is not adapted from previous Solar System photochemical models but derives from industrial applications (mainly combustion in car engines). Details about this chemical network and its range of validity are presented in Sect. 2.1.

We use this chemical network in a 1D model that includes photolyses and vertical transport, which has been previously used to study the atmospheric photochemistry of various objects of the Solar System: Neptune (Dobrijevic et al. 2010), Titan (Hébrard et al. 2006, 2007), Saturn (Dobrijevic et al. 2003; Cavalié et al. 2009), and Jupiter (Cavalié et al. 2008)) as well as extrasolar terrestrial planets (Selsis et al. 2002). We model the photochemistry of two hot Jupiters: HD 209458b and HD 189733b (Sect. 2.5). We study the departure from thermodynamic equilibrium and compare our results with those of Moses et al. (2011) (Sect. 3). We also investigate how including different reaction networks specific to nitrogen-bearing species influences the model results (Sect. 3.3) and the planetary synthetic spectra (Sect. 3.3.1).

2. The model

2.1. Kinetic network: from car engine to hot Jupiters

Significant progress has been done during the past decade in the development of validated combustion mechanisms. In the context of limiting the environmental impact of transportation, there is indeed a need in the development of detailed chemical kinetic models more predictive and more accurate for the combustion of fuels. One part of the studies undertaken in the LRGP (Laboratoire Réactions et Génie des Procédés, Nancy, France) concerns engine-fuel adaptation in order to improve the efficiency of engines and to limit the emission of pollutants. Gasoline and Diesel fuels contain a large number of molecules belonging to several major hydrocarbon families. Biofuels contain also oxygenated species, such as alcohols and methyl es-

---

[1] http://www.kinetics.nist.gov/kinetics

[2] In the field of combustion, a *mechanism* or reaction base is a network of reactions able to describe the kinetic evolution of a given pool of species. The mechanism includes the list of reactions and the associ-

ated rate coefficients, in a modified Arrhenius form, as well as the thermodynamic data for all the species involved in these reactions, which are required to calculate the equilibrium constants of the reactions and the rates of the reverse reactions

ters. Oxidation and combustion of these complex blends occur by radical chain reactions involving hundreds of molecular and radical species and several thousands of elementary reactions in the case of pure reference fuels such as n-heptane, iso-octane or cetane. The primary focus of the currently developed chemical models is to simulate the main combustion parameters (auto-ignition delay times, laminar flame speed, heat release), which are needed for the design of engines or burners, to estimate the fuel consumption, and to model the formation of some of the main regulated pollutants (carbon monoxide, nitrogen oxides, unburned hydrocarbons and particulate matter). Most of these kinetic models were developed for industrial applications and have been validated in a range of temperatures, from 300 to approximately 2500 K, and for pressures from 0.01 bar to some hundreds of bar. What is worth noticing is the similarity of these temperature and pressure ranges with the conditions prevailing in hot Jupiters atmospheres, in the very layers where they influence the observed molecular features. In addition, combustion mechanisms mainly deal with molecules made of C, H, O and N, which are also the main constituents of the molecules and radicals in these atmospheres. For this reason, we have decided to implement such a mechanism, which has already been applied successfully to many cases and systematically validated (Bounaceur et al. 2007), to study the atmosphere of hot Jupiters.

In this study we have used a C/H/O/N mechanism, whose core is a C_0-C_2 mechanism that includes all the reactions required to model the kinetic evolution of radicals and molecules containing less than three carbon atoms. This mechanism also contains some species with more carbon atoms that are needed to model the abundance of C_0-C_2 species. This mechanism does not include nitrogen species, except N_2 as a third body. As nitrogen species, such as N_2, NH_3, HCN, CN, are expected to be important constituents of hot Jupiter atmospheres, we completed this C_0-C_2 base with a validated sub-mechanism specifically constructed to model nitrogen species and all the cross-term reactions involved (for instance, reactions between alkanes and NO_X). These mechanisms do not use rate coefficients that have been adjusted by optimization procedures in order to fit experiments. Their values are those recommended for the individual processes by the main kinetics databases for combustion (Tsang & Hampson 1986; Manion et al. 2008; Smith et al. 1999; Baulch et al. 2005). The list of the reactions and their rate coefficients are available in the online database KIDA: KInetic Database for Astrochemistry[3] (Wakelam et al. 2012). The final mechanism includes 957 reversible and 6 irreversible reactions (see Sect. 2.1.3), involving 105 neutral species (molecule or radical). Helium is also included in this mechanism and plays the role of third body in some reactions.

2.1.1. C_0-C_2 reaction base

The C_0-C_2 reaction base we use was developed for industrial applications and was first presented by Barbé et al. (1995) and has been continuously updated (Fournet et al. 1999; Bounaceur et al. 2010). This mechanism is designed to reproduce the kinetics of species with less than three carbons. It includes all the unimolecular or bimolecular reactions involving radicals or molecules containing no more than two carbon atoms. This mechanism has been built by using a reaction grid, as proposed by Tsang & Hampson (1986). Every unimolecular and bimolecular elementary forward reactions involving the considered reacting species have been systematically written. Reacting

species include 46 compounds (19 molecules and 27 radicals) which have been ranked according to the molecular formula $O_xC_yH_z$ (with x varying from 0 to 3, y from 0 to 2 and z from 0 to 6): CO, H_2, H_2O, O_2, H_2O_2, CH_4, H_2CO, CH_3OH, CO_2, CH_3OOH, C_2H_2, C_2H_4, C_2H_6, CH_2CO, CH_3CHO, C_2H_5OH, C_2H_5OOH, CH_3COOOH, cC_2H_4O (Ethylene Oxide), C, CH, $^1CH_2$ (singlet), $^3CH_2$ (triplet), $O(^3P)$, H, OH, OOH, CH_3, HCO, CH_2OH, CH_3O, CH_3OO, C_2H, C_2H_3, C_2H_5, $CHCO$, CH_2CHO, CH_3CO, C_2H_5O, C_2H_4OOH, C_2H_5OO, CH_3COOO, CH_3OCO, CO_2H, 1-C_2H_4OH and 2-C_2H_4OH (ethyl radical isomers, 1-hydroxy and 2-hydroxy). This ranking permits to separate easily the part of the mechanism related to pyrolysis reactions from the one related to oxidation or combustion. The mechanism also includes 14 species containing 3 or 4 carbon atoms: C_3H_8, C_4H_8, C_4H_{10}, C_2H_5CHO, C_3H_7OH, C_3H_7O, C_4H_9O, C_2H_6CO, C_3H_8CO, C_2H_3CHO, n-C_3H_7, i-C_3H_7 (isopropyl and n-propyl radical isomers), 1-C_4H_9 and 2-C_4H_9 (1-butyl and 2-butyl radical isomers).

This C_0-C_2 mechanism has been widely validated in the 300-2500 K, 0.01-100 bar range for several types of reactors such as shock-tubes, perfectly stirred reactors, plug-flow reactors, rapid compression machines, laminar flames (e.g. Battin-Leclerc et al. 2006; Bounaceur et al. 2007; Anderlohr et al. 2010; Bounaceur et al. 2010; Wang et al. 2010). Obviously, it is not possible to describe in details all these validations, but we can mention, for instance, the very recent work of Dirrenberger et al. (2011) who has studied experimentally and modeled with success the laminar burning velocity of several mixtures including air, hydrogen and components of natural gas. Laminar burning velocities are important parameters in many areas of combustion science such as the design of burners and the prediction of explosions. They also play an essential role in determining several important aspects of the combustion process in spark ignition engines. These experiments have been done in specific mixtures, containing nitrogen in the sole form of N_2 and in which nitrogen species produced from N_2 (NO_X in the typical mixtures used in combustion) do not significantly affect the outcome, in order to validate the C_0-C_2 mechanism itself. Therefore, a model including only the C_0-C_2 base would not be accurate to predict the abundance of C_0-C_2 species in this range of P and T when applied to mixtures containing or producing (by reaction with N_2) significant levels of nitrogen species other than N_2.

2.1.2. Nitrogen reaction base

In our nominal model, the sub-network for the nitrogen bearing species is derived from Konnov (2000, 2009) and Coppens et al. (2007). It is based on a comprehensive analysis of the combustion chemistry of nitrogen oxides (Konnov & De Ruyck 1999a), ammonia (Konnov & De Ruyck 2000b), hydrazine (Konnov & De Ruyck 2001b), and modeling of nitrogen oxides formation in different combustion systems (Konnov & De Ruyck 1999b, 2000a, 2001a). The mechanism was tested at the California Institute of Technology, USA, and found suitable for steady one-dimensional detonation and constant volume explosion simulations (Schultz & Shepherd 1999). It was also preferred by the researchers at the University of Bielefeld, Germany to analyze flame structure and NO reburning in C_3 flames (Atakan & Hartlieb 2000). In addition, we consider a few additional pathways for HCN oxidation from Dagaut et al. (2008).

---

[3] http://kida.obs.u-bordeaux1.fr

Validations of our nominal sub-network for nitrogen bearing species have been made on the basis of experimental data obtained, for instance, by oxidation of HCN in a silica jet-stirred reactor (JSR) at atmospheric pressure and from 1000 to 1400 K (Dagaut et al. 2008), or studying laminar flame speeds in NH_3 - N_2O mixtures (Brown & Smith 1994). The nitrogen mechanism includes 42 species (molecule or radical): NO_3, $HONO_2$, CH_3ONO, CH_3NO_2, HNO_2, CH_3NO, NO_2, $HONO$, $HCNN$, $HCNO$, N_2O, NCO, HNO, $HOCN$, NNH, H_2CN, $N(^4S)$, CN, $HNCO$, NO, NH, NH_2, HCN, NH_3, N_2, N_2O_4, N_2O_3, N_2H_2, N_2H_3, N_2H_4, $HNNO$, $HNOH$, HNO_3, NH_2OH, H_2NO, CNN, H_2CNO, C_2N_2, $HCNH$, HNC, HON and NCN.

For comparison, we have also used other nitrogen sub-mechanisms, which are presented in Sec. 3.3 with the corresponding results.

Because the mechanism we use was created from individual processes and validated without any optimization of their reaction coefficients, its application outside the condition range of validation is not problematic. This is an issue, for instance, with the well-known combustion mechanism GRI-Mech 3.0[4] (Smith et al. 1999), proposed by Gas Research Institute, which is an optimized mechanism designed to model natural gas combustion. Optimization makes the model extremely accurate within the optimization domain but its application beyond is risky (Battin-Leclerc et al. 2011).

2.1.3. Reversible reactions: kinetics vs thermodynamics

For most reversible reactions, rate coefficients are only available for the exothermic (forward) direction. The rate constant for the endothermic (reverse) direction, $k_r(T)$ is then calculated as the ratio between the forward rate constant $k_f(T)$ and the equilibrium constant $K_{eq}(T)$, calculated with thermodynamical data, as explained in Appendix A. However, rate coefficients have sometimes been measured for both directions. In such cases, the ratio $k_f(T)/k_r(T)$ departs from $K_{eq}(T)$ as different uncertainties affect the rate coefficients and the thermodynamic data. The computation of $k_r(T)$ using $K_{eq}(T)$ ensures the consistency between kinetics and thermodynamics by making the kinetic model evolve strictly toward the thermodynamic equilibrium that we calculate. Nevertheless, this choice may not always be the best. It results in the propagation into $k_r(T)$ of both the errors affecting $k_f(T)$ and $K_{eq}(T)$. Indeed, thermodynamic parameters used to calculate $K_{eq}(T)$ are not free of error, and are regularly updated just as kinetic data. In the field of combustion, for small species as CH_4, CH_3 and OH, it is common to use experimentally measured kinetic rates, rather than thermodynamical reversal, when they are available in the relevant temperature range. There is no obvious rule in this matter, but validation of the mechanism with out-of-equilibrium experiments seems the only practical way to chose between different rates. This is the criterion that we use and our nominal network uses thermodynamical reversal for most of the reactions but not for three important ones. These reactions affect the unimolecular initiations (or thermal dissociation reactions) of methane into methyl and hydrogen radicals:

$$CH_4 \xrightarrow{M} CH_3 + H \tag{1}$$

of ethane into two methyl radicals:

$$C_2H_6 \xrightarrow{M} CH_3 + CH_3 \tag{2}$$
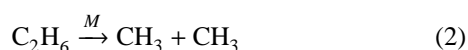
and of hydrogen peroxide into two hydroxyl radicals:

$$H_2O_2 \xrightarrow{M} OH + OH \tag{3}$$

At high temperature, chemical kinetics is very sensitive to these three reactions, which have been widely studied experimentally (Baulch et al. 1994; Golden 2008; Troe 2011). Therefore, we use the kinetic data measured experimentally for the forward and the reverse directions instead of calculating the reverse rate constants using thermodynamic parameters.

2.1.4. Excitation of oxygen and nitrogen atoms

Photodissociations produce excited states of oxygen ($O(^1D)$) and nitrogen ($N(^2D)$) that are not treated in the original combustion mechanisms. Therefore, we added to the C/H/O/N mechanism, 19 reversible reactions which describe the kinetics of $O(^1D)$ and $N(^2D)$, including radiative and collisional desexcitation. These reactions rates are taken (or have been estimated) from Okabe (1978); Herron (1999); Umemoto et al. (1998); Balucani et al. (2000a); Sato et al. (1999); Balucani et al. (2000b) and Sander et al. (2011).

2.2. Test on the chemical scheme with a 0D model

In addition to our 1D model, we have also developed a simple 0D model that computes the chemical evolution of a mixture at constant temperature and pressure. It does not include mixing with another mixture nor photolyses. We have used this 0D model to compare the composition found at steady state with the abundances at thermodynamic equilibrium (calculated with the code TECA, described in Appendix B) for several couples of pressure-temperature. Fig. 2 illustrates this comparison with four species. First, we used a version of our nominal scheme in which *all* the reactions are reversed in agreement with their equilibrium constant (solid lines). The computed abundances converge exactly towards the equilibrium values (dotted lines) with negligible numerical differences. Then, we used our nominal model in which some reactions are not reversed according to their equilibrium constant but using rate coefficients measured experimentally . In this case, the abundances reached at steady state (dashed lines) departs from the predicted equilibrium. This departure remains very small: below 1% for most species, and always below 5%. However, one can see that the kinetic evolution can be significantly different, both in terms of abundances and timescales.

2.3. The 1D model

To model the chemical composition of the atmosphere of the hot Jupiters HD 209458b and HD 189733b, we use our 1D time-dependent model described in Dobrijevic et al. (2010). As an input of the model, we give a pressure-temperature profile for the atmosphere of the planet studied. This profile is then divided in discrete uniform layers with a thickness $\Delta z = \frac{H(z)}{8}$, where $H(z)$ is the pressure scale height. The grid contains ~ 300 layers. Then the 1D kinetic model resolves the continuity equation (Eq. 4) as a function of time, for each species and atmospheric layer, until a steady state is reached.

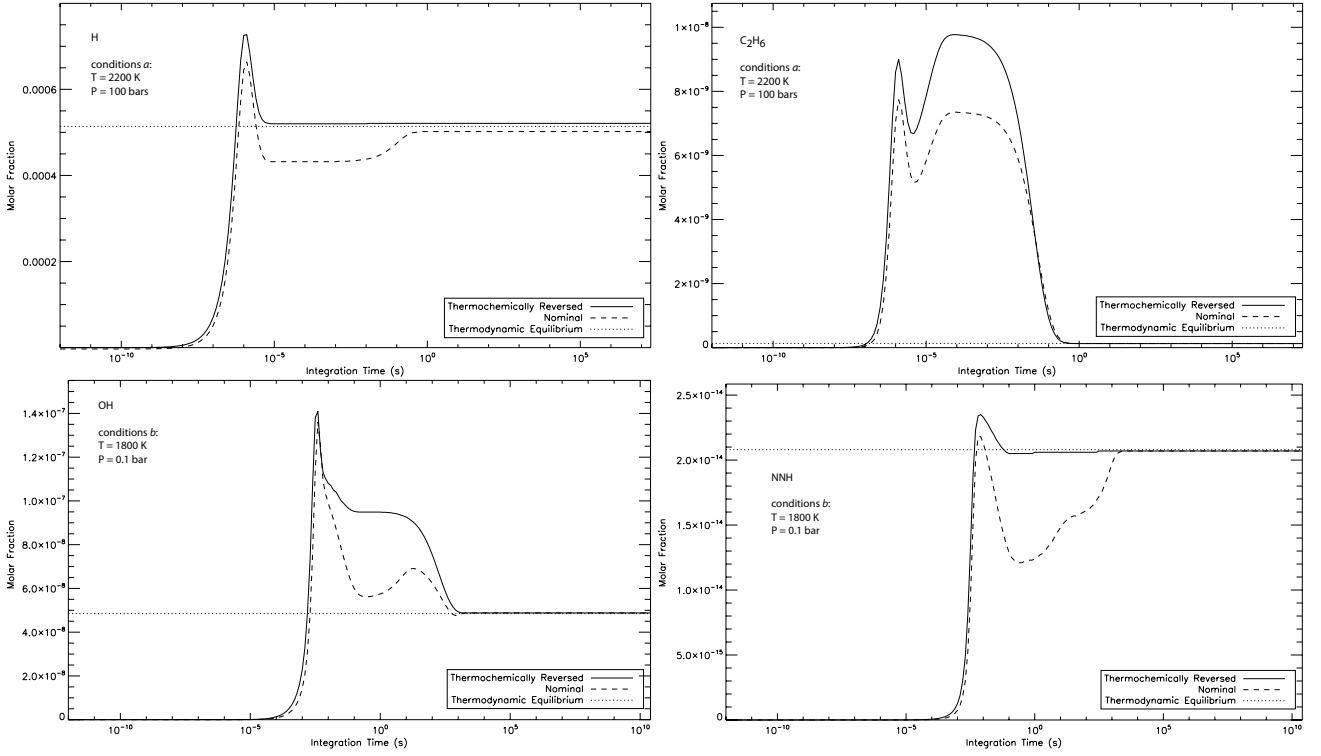$$\frac{\partial n_i}{\partial t} = P_i - n_i L_i - div(\Phi_i \vec{e_z}) \tag{4}$$

Fig. 2: Comparison between the thermodynamic equilibrium (dotted line) and the evolution of some molecular abundances in the 0D model, with two different schemes: the thermochemically reversed model (full line) and the nominal model (dashed line) as a function of integration time at different temperature-pressure points. Initial condition is a mixture of H_2, CH_4, O_2, N_2 and He with solar elemental abundances.

where n_i the number density of the species i (cm^{-3}), P_i its production rate (cm^{-3}.s^{-1}), L_i its loss rate (s^{-1}), and Φ_i its vertical flux (cm^{-2}.s^{-1}) that follows the diffusion equation:

$$\Phi_i = -n_i D_i \left[\frac{1}{n_i} \frac{\partial n_i}{\partial z} + \frac{1}{H_i} + \frac{1}{T} \frac{dT}{dz} \right] - n_i K \left[\frac{1}{y_i} \frac{\partial y_i}{\partial z} \right] \qquad (5)$$

where K is the eddy diffusion coefficient (cm^2.s^{-1}), D_i is the molecular diffusion coefficient (cm^2.s^{-1}) and H_i the scale height of the species i.

At both upper and lower boundaries, we impose a null flux for each species.

2.4. Photochemistry

We add to the thermochemical scheme a set of 34 photodissociations, which are presented in Appendix D. As we can see in Fig. 3, for HD 209458b and HD 189733b, UV flux penetrates down to a pressure of about 1 bar, where the temperature is higher than 1500 K. At these temperature and pressure, endothermic reactions do matter, which implies that photochemistry and thermochemistry are coupled in such highly irradiated atmospheres. We used absorption cross section at the highest available temperature (i.e. 370 K at maximum, which is low compared to the temperatures in the atmosphere of hot Jupiters (see Fig. 4)).

To calculate the photodissociation rates in all the layers of the atmosphere, we compute the stellar UV flux as a function of pressure and wavelength, taking into account molecular absorption by 22 species (Appendix D) and Rayleigh scattering. Actinic fluxes are calculated with a resolution of 1 nm
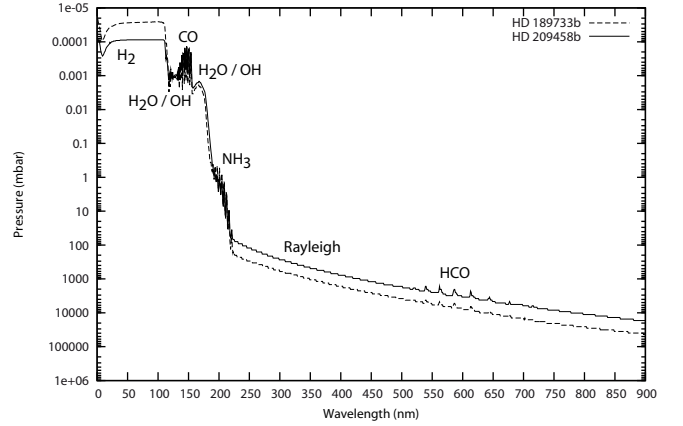

Fig. 3: Penetration of UV flux in the atmosphere of HD 209458b and HD 189733b at the steady state in function of wavelength. Plots represent the level where the optical depth $\tau = 1$. The name of the compounds responsible for the main absorption at different wavelengths is indicated.

(which is also the resolution we adopted for the absorption cross-sections), assuming a plane parallel geometry and an incidence angle θ of 48° (as done in Moses et al. (2011), because $< \cos \theta > = 2/3$ ($\theta \simeq 48°$) is the projected-areaweighted average of the cosine of the stellar zenith angle over the planetary disk at secondary-eclipse conditions). Multiple Rayleigh scattering is coupled with absorption through a simple two-stream iterative algorithm (Isaksen et al. 1977).

2.5. Application to hot Jupiters: HD 209458b and HD 189733b

HD 209458b and HD 189733b are transiting planets around nearby bright stars. Their atmospheres have been studied by their transmission spectrum obtained during the primary transit and their day-side emission spectrum measured at the secondary eclipse. These observations can be used to constrain the thermal profile (Swain et al. 2009a; Madhusudhan & Seager 2009) and to detect the spectral signature of atmospheric compounds (Charbonneau et al. 2002; Tinetti et al. 2007; Swain et al. 2008b; Grillmair et al. 2008; Langland-Shula et al. 2009; Swain et al. 2009a,b; Beaulieu et al. 2010).

In this preliminary study, we do not compare the results of our model with these observations for two reasons. First, because there is not yet a consensus on the actual constraints that can be drawn from these measurements. Secondly, such a comparison would imply to address the effects of circulation on the composition and to explore all the range of possible elemental abundances for these objects. Several recent works claim that observations of some hot Jupiters imply enhanced elemental C/O ratios (Madhusudhan et al. 2011a,b). With C/O ratios close or above unity, species with more than two carbon atoms will be important and our C_0-C_2 network does not allow us to study them. For these reasons, we are implementing a C_0-C_6 mechanism and a coupling with atmospheric circulation, which will be described in further studies. At this stage, our main goal is to compare the results of our model with already published works, in particular Moses et al. (2011), hereafter M11. We could also have compared our results with those of Zahnle et al. (2009a), who explored a broader range of conditions, included sulfur-bearing species and various elemental compositions. We decided to restrict our comparison with M11 because their model, like ours, only includes species made of C, H, O and N (and He), and also because M11 already did a comparison between their results and those of Zahnle et al. (2009a) showing only little discrepancies when the same conditions are considered. We used the same conditions (*P-T* profiles, eddy diffusion, elemental abundances) as in M11, so that differences should come only from kinetics (and photochemistry in the upper atmosphere), which represents the novelty of our approach.

2.5.1. Physical properties and composition

The physical properties of HD 209458b have been refined by Rowe et al. (2008) and are presented in Table 1, with some properties of the host star. Properties of HD 189733b and HD 189733 come from Southworth (2008, 2010).

In order to compare the outcomes of the two models (Sect. 3.2), we use the temperature and eddy diffusion profiles published in M11 (Figs. 4). Also following M11, we assume protosolar elemental abundances (Lodders & Palme 2009) for both planets, with 20% of depletion for oxygen (sequestered along with silicates and metals). We start our time-dependent modeling with the thermodynamic equilibrium abundances calculated with TECA (an equilibrium model described in Appendix B) at each level of the atmosphere.

2.5.2. UV spectral irradiance

As HD 209458 is a G0 star (Table 1), we use the UV spectral irradiance of the Sun for this star. For the star HD 189733, a K1 - K2 star (Table 1), the UV spectrum has been provided

Table 1: Properties of the systems HD 209458 and HD 189733

	HD 209458	HD 189733
Distance Sun-Star (pc)	47	19.3
Distance Planet-Star (AU)	0.047	0.03142
$M_p(M_{Jup})$	0.69 ± 0.01	1.150 ± 0.028
$R_p(R_{Jup})$	1.339 ± 0.002	1.151 ± 0.036
$\rho_p(\rho_{Jupiter})$	0.26 ± 0.04	0.755 ± 0.066
$g_0(m.s^{-2})$	9.54 ± 0.69	21.5 ± 1.2
P_{orbit} (days)	3.5247489(2)	2.21857578(80)
$M_\star(M_\odot)$	1.083 ± 0.005	0.840 ± 0.030
$R_\star(R_\odot)$	1.118 ± 0.002	0.752 ± 0.023
Spectral type	G0 V	K1 V - K2 V

NOTE.– The 1σ uncertainty in P_{orbit} is given in parentheses in units of the last digits

to us by Ignasi Ribas (private communication). It is based on FUSE and HST observations of the star ϵ Eridani, a proxy of HD 189733 (similar type, age and metallicity), in the 90-330 nm range. Between 0.5 and 90 nm, it is based on data from the X-exoplanets Archive at the CAB (Sanz-Forcada et al. 2011). Above 330 nm, we use a synthetic spectrum calculated with the stellar atmosphere code Phoenix (Hauschildt et al. 1999). This model for the UV spectrum of HD 189733 slightly differs from the one chosen in M11. We also tested our model with the spectrum used by M11 and found negligible differences at the pressure levels we model.

3. Results

3.1. Nominal model

First of all, we checked that our kinetic model reproduces the thermodynamic equilibrium, in the absence of vertical mixing and photodissociation. We obtained differences lower than a few percent, as found with the 0D model (see Sect. 2.2). For both planets, the homopause is always found above the 1×10^{-5} mbar level, which is beyond the range of pressure that we model. As a consequence, and although it is included, molecular diffusion does not affect our results.

Figure 5 shows the steady-state composition of the atmosphere of HD 209458b and HD 189733b, with vertical transport and photodissociations, while in Fig. 6, photodissociations have been removed. Comparing Figs. 5 and 6 shows us the influence of photolyses. Although HD 209458b receives a higher UV flux than HD 189733b, we can see that UV photons have little effect on the composition of HD 209458b, while they have a significant influence on the chemistry of HD 189733b. This is because the temperature is higher in HD 209458b so that the chemical timescales are significantly shorter than the lifetime of species against photolyses. So in HD 209458b, kinetics dominate over photodissociations, even at high altitude. In HD 189733b, however, photodissociations affect the composition down to about the 10 mbar level. This is particularly noticeable for H and OH abundances. The production of H is dominated by the photolysis of H_2 for pressures lower than 1 μbar. Below this level, and for pressures higher than 0.1 mbar, H is produced by the photodissociation of H_2O, with a minor contribution of the photodissociations of NH_3 and HCN. The abundance of OH follows the profile of H, and increases for pressures lower than 10 mbar. There is a photochemical enhancement of HCN above the 10 mbar pressure level, as discussed in M11. CH_4 is destroyed by photolyses for pressures lower than 0.01 mbar. NH_3 is photodissociated down to levels as deep as 1 bar, but vertical transport
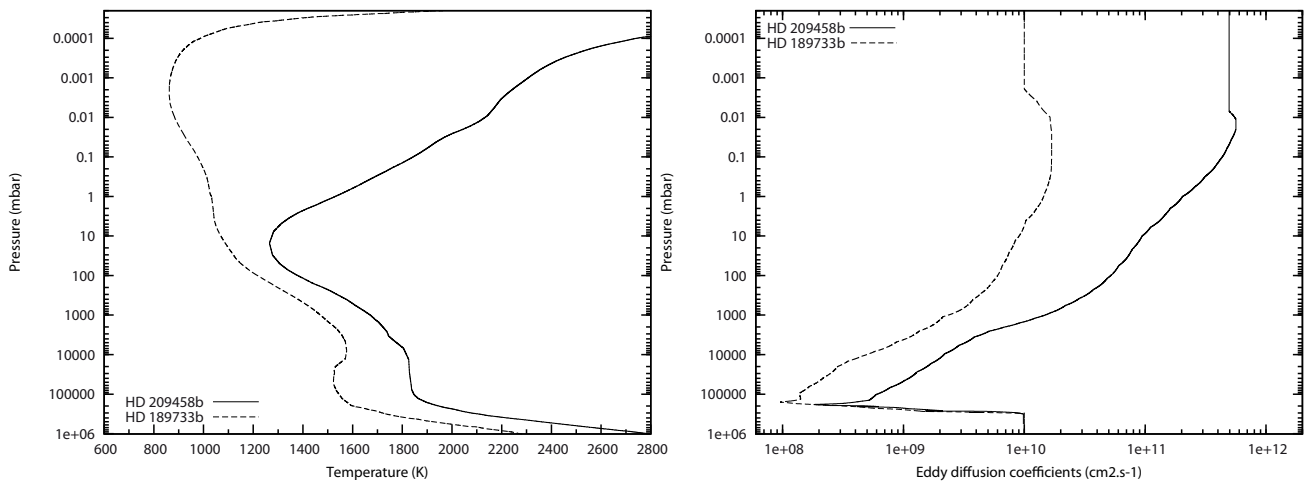
Fig. 4: Pressure-temperature profiles (left) and eddy diffusion profiles (right) of HD 189733b and HD 209458b (from Moses et al. 2011).

compensates this destruction for pressures higher than 0.1 mbar. Above that level, the amount of NH_3 decreases with altitude due to photolyses. Photochemistry has a negligible effect on CO_2, as noted by Zahnle et al. (2009a).

For HD 209458b, we can see in Fig. 6 that mixing quenches NH_3 and HCN at 1 bar and CH_4 at 400 mbar. These species are transported up to ~1 mbar pressure level, but as the temperature increases with altitude at this level, they tend to come back to their thermochemical equilibrium values, so their abundances decrease again. For the other molecules, like H_2, H and CO_2, at the thermodynamic equilibrium, there is a steep variation of composition (smoothed by vertical mixing) corresponding to the strong temperature gradient of the upper atmosphere.
Vertical quenching has an effect on a larger part of the atmosphere of HD 189733b. NH_3 and HCN are quenched at 5 bar, CH_4 at 1 bar, H at 40 mbar and CO_2 at 20 mbar. Quenching contaminates the composition up to very low-pressure levels (10^{-4} mbar).

3.2. Comparison with Moses et al. (2011)

3.2.1. Equilibrium

Overall, the composition we calculate at thermodynamic equilibrium (which is our initial condition) is very close to what is obtained by M11 except for HCN for which there is a difference that can reach ~ 30% at 100 bars and 1545 K. To check our calculations we also did a comparison with the code STANJAN[5] and we found negligible discrepancies for the species we compared, including HCN at this pressure and temperature. The difference with M11 probably comes from the coefficients used for the NASA polynomials (see Appendix A). Although the difference remains small for equilibrium calculations, we should keep in mind that it may significantly affect the kinetics of HCN and related species through the calculation of the rate for backward reactions and vertical quenching.

3.2.2. Steady-state

In Fig. 7, we compare our results at steady state with those of M11. Differences between M11 and our nominal model are

also shown species by species in Figs. 8 and 9. Discrepancies between the two models can be due to the different chemical schemes and, at levels where the results are sensitive to photochemistry, to possible differences in the UV fluxes, cross sections, and photodissociation quantum yields. An influence of the numerical implementation (like the discretization of the atmosphere, the solver for the continuity equations, or the treatment of the UV transfer) is also possible.

In the lower atmosphere of HD 189733b and for most of the atmosphere of HD 209458b, photolyses have a negligible influence and departures should be caused by the kinetics. For these regions we find very similar results for species that remain at their equilibrium abundance (H, OH, CO, CO_2, H_2O for instance), which only confirms, as stated before, that our thermodynamic equilibrium codes are in good agreement. For species quenched by mixing, however, significant deviations appear, in particular for NH_3, HCN and CH_4. Their quenching occurs at different pressure levels and, thus, for different abundances that will then contaminate a large fraction of the atmosphere above. The discrepancies are much more significant in the case of HD 189733b, due to a higher sensitivity to kinetics. Although the kinetic network is certainly the main reason for these departures, it is also true that quenching can be quite sensitive to the resolution of the pressure (or altitude) grid, in particular when there is a steep gradient of temperature which is the case in the convective zone (P >100 bar). For this reason, we impose the thickness of individual layers to be smaller than $1/8^{th}$ of the local scale height, which results in ~300 layers for the pressure range that we model. Although we do not know what resolution is used in M11, it seems more likely that the deviation comes from differences in the kinetic network itself. As explained in the Introduction, we use a chemical scheme validated for the species represented and for most of the range of temperature and pressure of the modeled atmospheres. M11, on the other hand, use a chemical scheme derived from Jupiter and Saturn models (Gladstone et al. 1996; Moses 1996; Moses et al. 1995b,a, 2000a,b) completed by high-temperature kinetics from combustion-chemistry literature (Baulch et al. 1992, 1994, 2005; Atkinson et al. 1997, 2006; Smith et al. 1999; Tsang 1987, 1991; Dean & Bozzelli 2000), which has not, to our knowledge, been validated against experiments. We also note departures in the upper atmosphere, where photolyses are important. In particular, H and OH exhibit similar

---

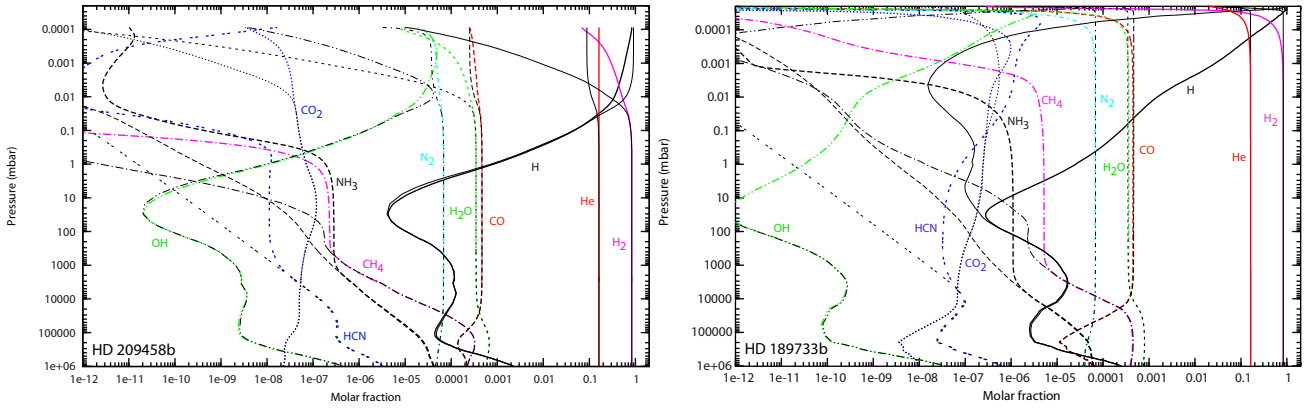[5] http://navier.engr.colostate.edu/tools/equil.html

Fig. 5: Steady-state composition of HD 209458b (left) and HD 189733b (right) calculated with our nominal model (color lines), compared to the thermodynamic equilibrium (thin black lines).
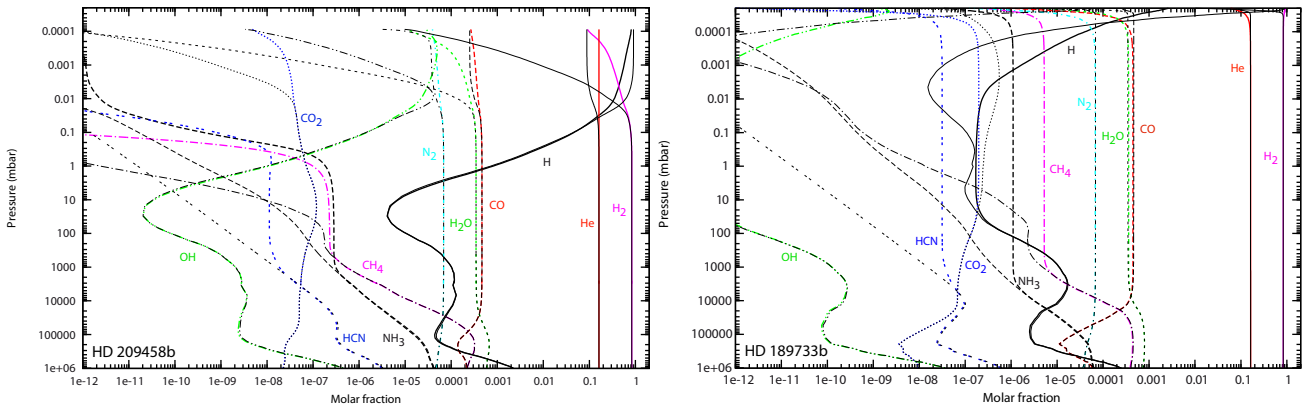

Fig. 6: Steady-state composition of HD 209458b (left) and HD 189733b (right) calculated with our nominal model without photodissociation (color lines), compared to the thermodynamic equilibrium (thin black lines).
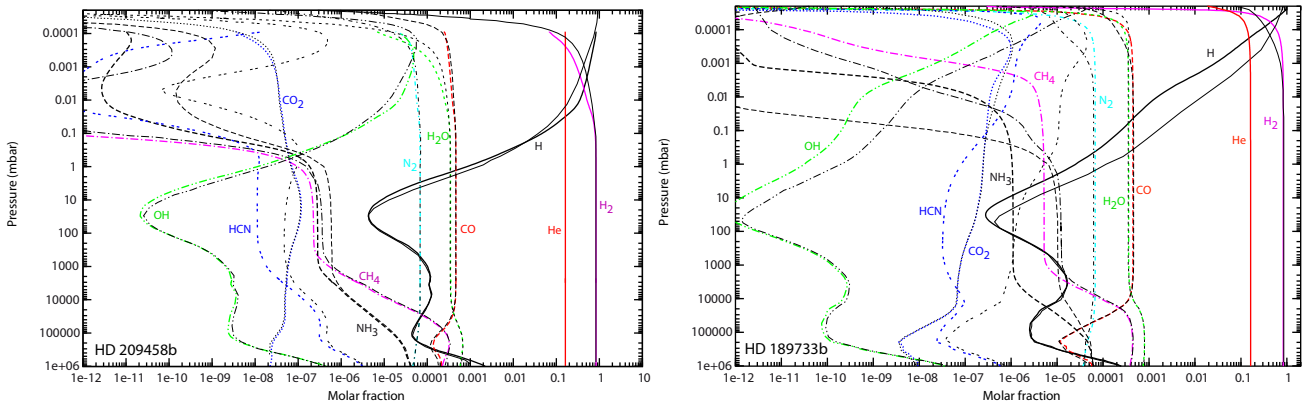

Fig. 7: Comparison between the abundance profiles found by our nominal model (color lines) and by Moses et al. (2011) (thin black lines), for the two planets (HD 209458b (left) and HD 189733b (right))

profiles than those of M11 in HD 189733b but shifted by about one order of magnitude in abundance for pressures lower than 50 mbar. CH_4 is also affected. We checked that these differences are not due to the use of different stellar fluxes by switching between the flux we use and the one used in M11 (for HD 209458b, we both use the solar UV flux). At these altitudes, we note a significant sensitivity of the mixing ratio of these species to the Rayleigh scattering, so the treatment of the scattering could ex-

plain at least part of this disagreement. Again, and although we do not know the details of the photochemical data and radiative transfer used in M11, we assume that kinetics explain the differences.

### 3.3. Other networks for nitrogen species

The main differences between M11 and our results is related to the quenching of NH$_3$ and HCN. As mentioned in M11, the chemistry of nitrogen compounds has been less studied than carbon species and chemical networks have been subjected to less validation. However, NO$_X$, HCN, CN and NH$_3$ are important species in applied combustion (gas fuel, for instance, can contain high concentrations of ammonia), and should be well reproduced within the temperature and pressure range of the validation. Quenching is found to occur within 1 to 10 mbars, corresponding to the range of validation in terms of pressure. An originality of our network compared to other schemes used in combustion is that it is not optimized to increase the agreement between modeling and experiments. In other words, the rate coefficients of the individual processes have not been altered compared to their original measurement or estimate. The application of the network is therefore not strictly restricted to the validation domain.

Other sub-mechanisms are available to model the kinetics of nitrogen-bearing species. They have been constructed based on different approaches (optimization, specific domain of application, reduced number of reactions). In order to test our model against other nitrogen schemes, we replaced our nitrogen reaction base by nitrogen sub-mechanisms taken from other C/H/O/N mechanisms:

- *GRIMECH*, mechanism based on GRI-Mech 3.0 (Smith et al. 1999) with several reactions involving NO$_X$ compounds added with respect to the mechanisms of Glaude et al. (2005) as recommended and done by Anderlohr et al. (2009). It includes 162 reversible reactions involving 26 nitrogen compounds. The GRI-Mech 3.0 is a mechanism designed to model natural gas combustion, including NO formation and reburn chemistry. As already mentioned in Sect. 2.1.2, it has been optimized as a global mechanism, i.e., some rate coefficients have been modified (relatively to the literature) in order to fit the results of a pool of experiments with conditions and compositions specific to combustion. The individual processes have not been studied separately in all the pressure and temperature range. Applying this mechanism beyond its domain of optimization/validation is a risky extrapolation. Mixing ratios of oxidants, for instance, are very low in hot Jupiter atmospheres compared with the experiments used to optimize/validate GRI-Mech 3.0.

While doing the present study, we noticed that two reactions from the *GRIMECH* mechanism had wrong rates and corrected them. These erroneous rate constants, that can be traced back to the NIST Chemical Kinetics Database (Manion et al. 2008), were identified by systematically comparing reaction rate constants with collision limit values and energy barriers with the enthalpy budget of the reaction.

The first reaction is

$$N_2 + H \longrightarrow N(^4S) + N(^4S) + H \qquad (6)$$
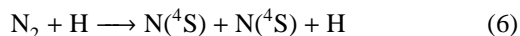
for which the rate given by NIST is $k_f(T)$=1.26 $\times$ 10^{-9} $T^{-0.20}$e$^{-27,254/T}$ cm^3 molecule^{-1} s^{-1} (with T in Kelvin), although this expression corresponds in fact to the reaction 7, the thermal dissociation of NH through collisions with atomic nitrogen (Caridade et al. 2005):

$$NH + N \longrightarrow H + N_2 \qquad (7)$$
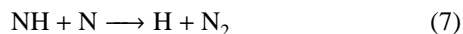
The above expression overestimates by many orders of magnitude the rate constant of the reaction, whose activation energy must be around 100,000 K, as implied by the bond energy of molecular nitrogen and by measurements of the thermal dissociation of N$_2$ through collisions with various bodies.

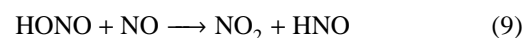We finally adopted for the dissociation of N$_2$ a more general form:

$$N_2 + M \longrightarrow N(^4S) + N(^4S) + M \qquad (8)$$
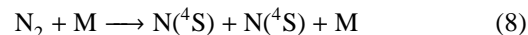
with the reaction rate constant $k_f(T)$=1.661 $\times$ 10^4 $T^{-3.30}$e$^{-11,310/T}$ cm^3 molecule^{-1} s^{-1} (Thielen & Roth 1986). This rate had a strong influence on our results. Note that using the wrong rate has a large effect on the atmospheric profiles of NH$_3$ and HCN.

The second reaction is

$$HONO + NO \longrightarrow NO_2 + HNO \qquad (9)$$

for which the reaction rate constant given by NIST ($k_f(T)$=7.34 $\times$10^{-20} $T^{2.64}$ e$^{-2034/T}$ cm^3 molecule^{-1}s^{-1}) was in fact the rate of the reverse of reaction (9), as calculated by Mebel et al. (1998). In our model, we use in fact the reaction :

$$NO_2 + HNO \longrightarrow HONO + NO \qquad (10)$$

with the reaction rate constant $k_f(T)$=1.00 $\times$10^{-12} e$^{-1000/T}$ cm^3 molecule^{-1}s^{-1} (Tsang & Herron 1991).

When this paper is published, these rates should be corrected in the NIST Chemical Kinetics Database, but one should check that the wrong rates are not used in modeling.

- *GDF-Kin*, a mechanism optimized for natural gas combustion modeling (Turbiez et al. 1998; De Ferrieres et al. 2008) that includes less individual processes: 180 reversibles reactions involving 22 nitrogen species. Several experimental data on natural gas combustion have been acquired in partnership with *Gaz de France* to develop this mechanism. NO$_X$ chemistry has been included in GDF-Kin 3.0 (El Bakali et al. 2006). We use the update version GDF-Kin 5.0 (Lamoureux et al. 2010), in which 5 reactions involving NCN have been refined in order to better reproduce the kinetics of this species. It is validated for temperatures between 400 and 2200 K and pressures between 0.04 and 10 bars.

- *DEAN*, taken from Dean & Bozzelli (2000). This book that presents a catalog of reactions is used by Moses et al. (2011), at least for some reactions. The mechanism derived from this work includes 370 reversible reactions involving 49 nitrogen species and one C/H/O species that is not included in our C$_0$-C$_2$ scheme: HCOH. The purpose of the work of Dean and Bozzelli was to list gas phase reactions involving nitrogen-bearing species that could be important for high temperature combustion modeling and to provide the associated rate coefficients based on an analysis of elementary reaction data, when available, or on estimations from thermochemical kinetics principles otherwise. This mechanism was developed on the basis of analysis of individual reactions rather than by attempting to reproduce any specific set of experiments. It is clearly written in this book that: "Although we show in the chapter that this mechanism provides a reasonable description of some aspects of high-temperature nitrogen chemistry, we have not attempted a comprehensive comparison". Therefore, this kinetic network should be viewed as a database
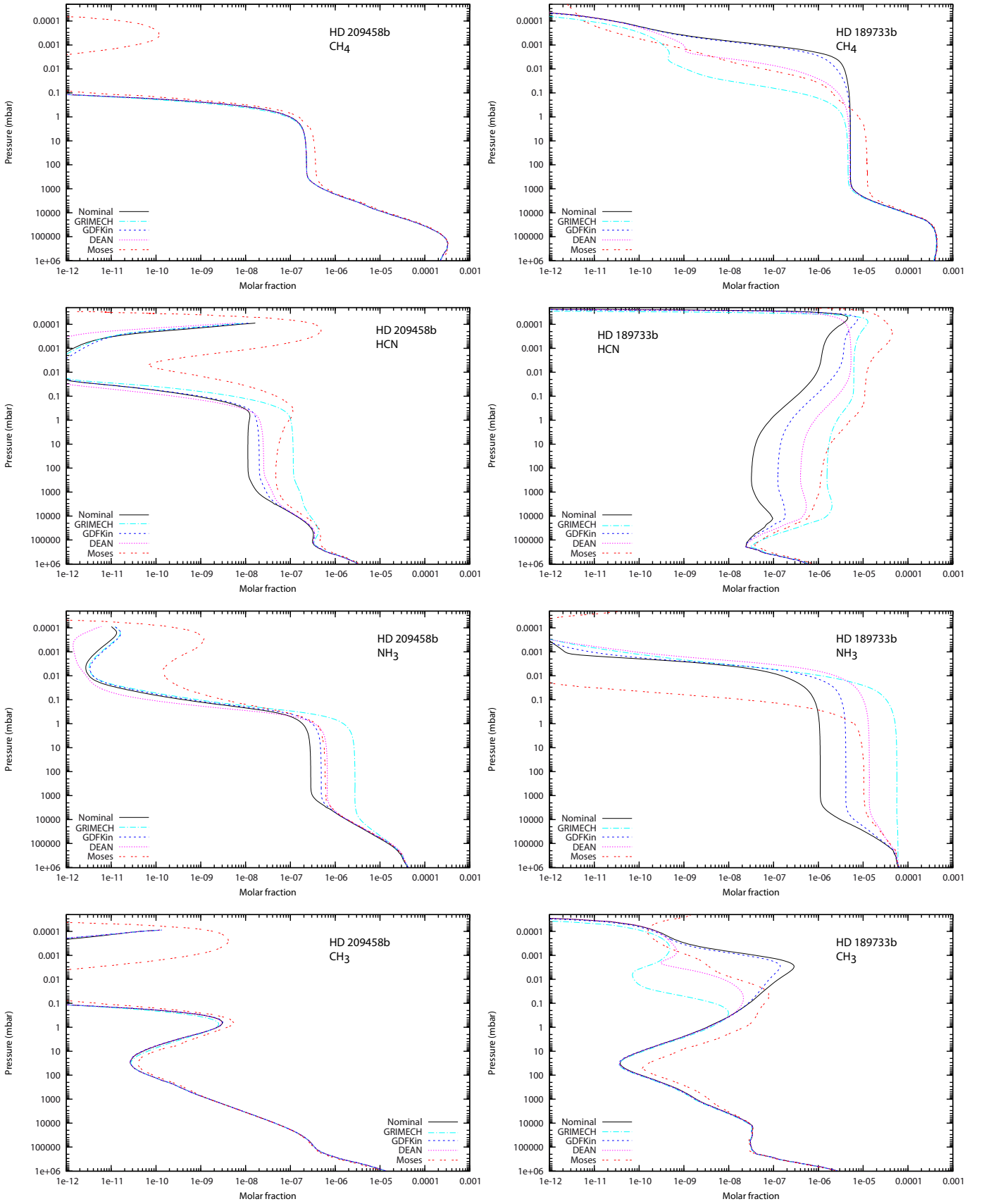
Fig. 8: Abundances of CH$_4$, HCN, NH$_3$ and CH$_3$ in HD 209458b (left) and HD 189733b (right) with the four different models, compared to the results of Moses et al. (2011).
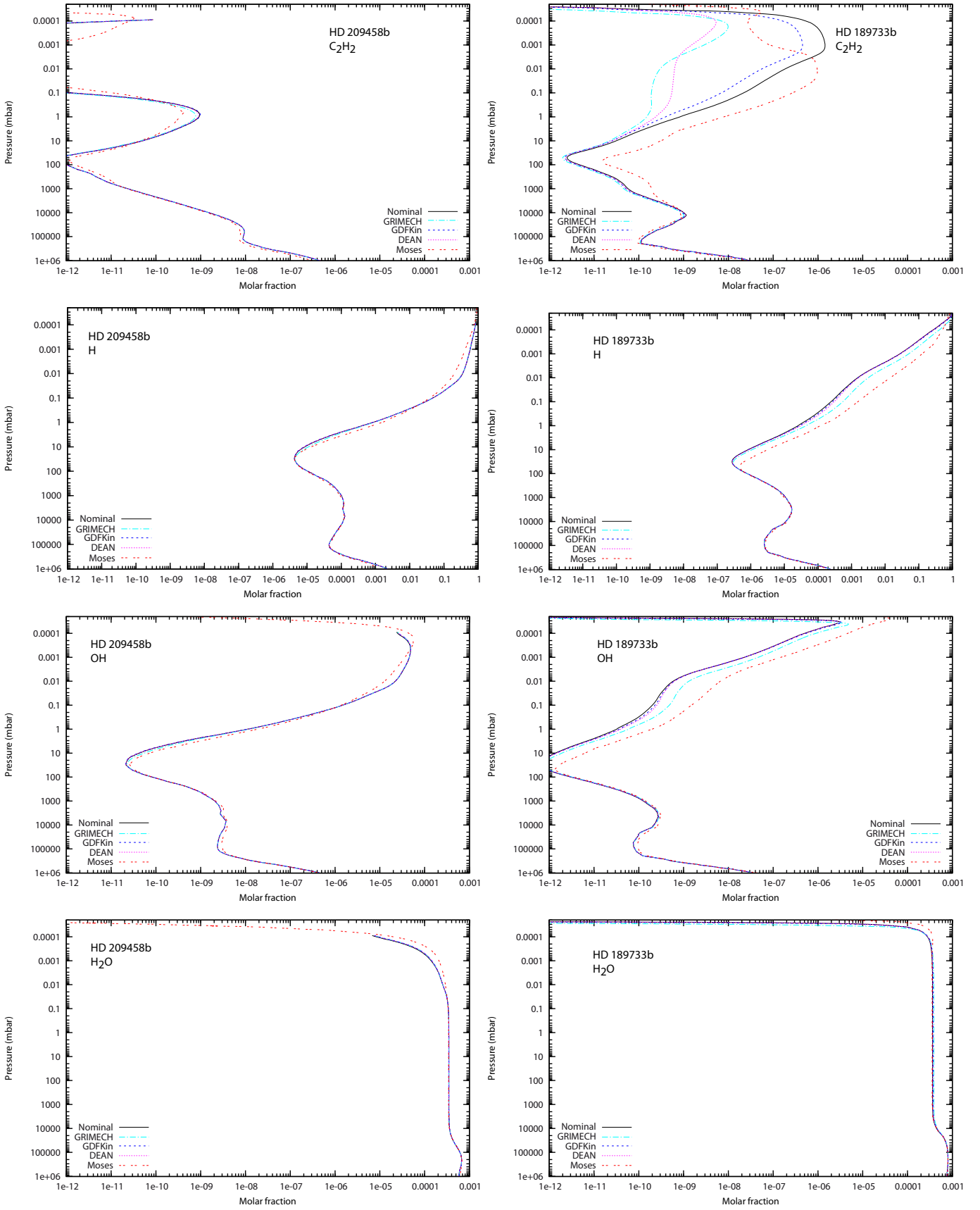
Fig. 9: Abundances of C_2H_2, H, OH and H_2O in HD 209458b (left) and HD 189733b (right) with the four different models, compared to the results of Moses et al. (2011).

of reaction rate constants rather than a validated mechanism, in the absence of validation.

The impact of the different nitrogen sub-mechanisms on the abundance profiles of various species is illustrated in Figs. 8 and 9. Thermodynamic equilibrium is the same for all schemes (for the species in common).

First, we restrict our analysis to pressures higher than ∼ 1 mbar in order not to mix effects due to kinetic rates with possible differences in the photochemical data or modeling. For HD 209458b, the main species that are significantly affected at these pressure levels by the change of nitrogen scheme are HCN and NH_3. This is not surprising as these are the most abundant nitrogen species departing from equilibrium due to quenching, and the pressure level at which the quenching occurs depends on the kinetic network adopted. These two species (but also others) show even larger differences in the case of HD 189733b, as the lower temperatures of this atmosphere enhance the differences due to the kinetics. Departures between schemes are expected to become even more important for cooler atmospheres. None of the tested schemes shows an general improvement of the agreement with M11. Similar NH_3 quenching is found by M11 and with *DEAN* for both planets, which makes sense as M11 use Dean & Bozzelli (2000) as a source of reactions and associated rates for N-bearing compounds. This similarity is found also for HCN but only at pressures higher than 1 bar. At higher altitudes, the HCN profiles from M11 become closer to the result with *GRIMECH*. For both planets and both HCN and NH_3, profiles obtained with *GDF-Kin* are bracketed by those from the nominal model and *DEAN*, while *GRIMECH* gives significantly higher abundances than all other models in the quenching region. With *GRIMECH*, we also notice that NH_3 becomes the main nitrogen-bearing species from the bottom of the atmosphere up to 0.03 mbar because of vertical mixing, whereas thermodynamics predicts that N_2 should be the main nitrogen-bearing species.

Understanding the roots of theses discrepancies would require an in-depth study of the sensitivities of these schemes to reaction cycles, as a function of temperature and pressure, which is far beyond the scope of this study and would require tools that may have to be developed specifically for such large networks. To illustrate this difficulty let us identify the reaction that dominates the production rate of NH_3 for HD 189733b, at 100 mbar. We find it to be the same for all mechanisms:

$$NH_2 + H_2 \longrightarrow NH_3 + H, \qquad (11)$$
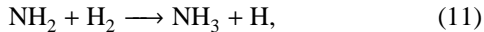
whose rate constant is similar in all schemes, and is calculated reversing the reaction:

$$NH_3 + H \longrightarrow NH_2 + H_2, \qquad (12)$$
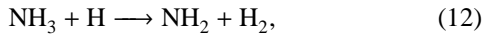
which dominates the destruction of NH_3, also in all the schemes. The following rates are found in the different schemes:
- Nominal, *Dean, GRIMECH*: $9.00 \times 10^{-19}T^{2.4}e^{-4990/T}$ $cm^3.molecule^{-1}.s^{-1}$, derived from Ko et al. (1990).
- *GDF-Kin*: $1.056 \times 10^{-18}T^{2.39}e^{-5114/T}$ $cm^3.molecule^{-1}.s^{-1}$ from Michael et al. (1986).
We could think that these slight differences are responsible for the different results. However, NH_3 does not display the same abundance when using *Dean* and *GRIMECH* mechanisms, despite the fact that they both share the same rate constant. Moreover, nulling the rate constant of this reaction in the nominal scheme, does not affect the quenching level of NH_3, nor its abundance for pressures higher than 10 mbar. We can therefore eliminate this hypothesis. Key reactions are in fact usually

those that limit the rate of a cycle and that do not dominate the production or destruction of a given species. Finding those limiting processes in complex networks is a field of research in itself. Identifying key pathways and their limiting reactions require dedicated algorithms (Lehmann 2004; Grenfell et al. 2006; Dobrijevic et al. 2010; Stock et al. 2011, 2012) whose adaptation to the large networks we consider will require further work.

For hydrocarbons (see for instance CH_4, C_2H_2 and CH_3) all the models we tested cluster to the same profiles for pressures below 1 mbar. This shows that N-bearing species have little influence on hydrocarbon chemistry at these altitudes. (This would no longer be true at higher temperature and for higher C/O ratios as HCN would become a major reservoir of both N and C). M11 systematically finds higher mixing ratios for hydrocarbons (but within one order of magnitude) above the quenching level of CH_4 (1-10 bar), likely due to kinetic differences in the C_0-C_2 mechanism.

At lower pressure, Figs. 8 and 9 show large differences that are no longer due to quenching. At pressures lower than 1 mbar, the abundances of hydrocarbons depend on the nitrogen network used. It is particularly striking for C_2H_2 in HD 189733b, where *DEAN* and *GRIMECH*, on the one hand, and the nominal model, *GDF-Kin* and M11, on the other hand, seem to cluster in two different regimes, exhibiting 2 to 3 order of magnitude differences at 0.1-0.001 mbar. Departures between network results can be due to differences in the kinetic network (different reactions, different rates, different minor species included) but also in photochemistry. Indeed, some UV-absorbing species are not included in all the models, such as N_2H_4, HNO_3, C_2N_2 and N_2O_4, which have absorption domains that overlap that of C_2H_2.

3.3.1. Corresponding emission and transmission spectra

In order to calculate the planetary transmission and emission+reflection spectra of HD 189733b (Fig. 10) and HD 209458b, we use a line-by-line radiative transfer model from 0.3 to 25 μm (Iro et al. 2005; Iro & Deming 2010). The opacity sources included in the model are the main molecular constituents: H_2O, CO, CH_4, NH_3, Na, K and TiO; Collision Induced Absorption by H_2 and He; Rayleigh diffusion and H^- bound-free and H_2^- free-free. For absorbing species not included in our kinetic model (Na, K and TiO), chemical equilibrium is assumed. The current model does not account for clouds. For the reflected component, we use synthetic stellar spectra generated from ATLAS[6]. The main difference from the static model described in Iro et al. (2005) is the addition of NH_3 for which we used the HITRAN 2008 database (Rothman et al. 2009). Planetary parameters are taken from Table 1.

We applied this model for the compositions obtained with the two nitrogen mechanisms, which give the most opposite results (Nominal and *GRIMECH*), as well as for chemical equilibrium. The *GRIMECH* scheme gives the highest abundance for ammonia: ten and one hundred times more NH_3 than the nominal model for HD 209458b and HD 189733b, respectively. As a consequence, features of this molecule become noticeable on both the emission and transmission spectra at 1.9, 2.3, 3.0, 4.0, 6.1 and 10.5 μm. The most prominent feature is found for HD 189733b at 10.5 μm. NH_3 features are also visible on the spectra of HD 209458b, but so slightly that it would not be observable.

At the moment, our radiative transfer model does not include the contribution of HCN to the opacities. Based on the HCN

---

[6] http://kurucz.harvard.edu/stars.html

abundances and associated spectra found by M11, we can expect the spectra to be also sensitive to the HCN abundance. Indeed, at the altitudes probed by the observations, there is nearly two orders of magnitude less HCN with our nominal model than with *GRIMECH*, and *GRIMECH* gives HCN abundances similar to that of M11. Therefore, the signature of HCN found by M11 at 14 μm should also become noticeable with the *GRIMECH* version of our scheme.

Some observational data are superimposed to the spectra (Charbonneau et al. 2008; Grillmair et al. 2008; Swain et al. 2009b) (for emission spectrum) and (Knutson et al. 2007, 2009; Swain et al. 2008b; Beaulieu et al. 2008; Sing et al. 2009; Désert et al. 2009; Agol et al. 2010) (for transmission spectra), but we do not discuss the agreement between observations and synthetic spectra, as we did not attempt to fit the observable using different thermal profiles.

4. Discussion

To study HD 209458b and HD 189733b, we use the pressure-temperature and eddy diffusion profiles from M11. These profiles are derived from general circulation models of Showman et al. (2009). This choice is motivated by the comparison with M11 and also because the actual physical structure of these atmospheres is not yet well constrained by observations. Note however, that Huitson et al. (2012) recently published thermal profiles for both planets, as inferred from transit spectroscopy. It seems that HD 189733b could be warmer than HD 209458b between 10^{-5} and 10^{-3} bar. Considering the large uncertainties affecting their physical conditions, our models should not be considered as predictions of the composition of hot Jupiters but more as a step in developing chemical models of these objects and model intercomparison.

In addition, circulation is not included in our model nor, to our knowledge, in other current photochemical models of hot Jupiters although it has a significant influence on the chemical composition of the atmospheres due, for instance, to the strong longitude dependency of the temperature. We study the influence of the horizontal transport on the composition of the atmosphere of HD 209458b in a forthcoming paper (Agúndez et al., in preparation).

Because modeled abundances depend significantly on the reaction network (in particular for NH_3, HCN and some hydrocarbons), we recommend using a network that has been validated (but not optimized) against experiments for conditions as close as possible to those of application. We do not claim that the network we release is a definitive one, it will necessarily evolve as new experimental results and kinetic/thermodynamic data become available. Detailed nitrogen chemistry, for instance, has been implemented in combustion networks only recently and will be subjected to further evolution. Missing elements should also be added to the network, sulfur being the most obvious one. Since the scheme has not been optimized, adding new species and reactions to the network we release is possible. Moreover, although the range of *P*, *T* and the elements considered in combustion model do fit well with the study of hot Jupiter atmospheres, the ratio between hydrogen and the other elements does not. For this reason, among others, it is important to avoid using optimized networks that would prevent modeling of such hydrogen-rich mixtures. Note also that our current network, that cannot be used to study the abundance of species with more than 2 carbon atoms, is likely insufficient to study atmospheres with C/O ratios close to or above unity. For this reason we are currently working on an extended network that can model species up to 6 carbon atoms.

Hot Jupiter atmospheres represent an extreme case of planetary atmospheres in terms of both high temperatures and low metallicity. With the progress of observations, cooler and heavier atmospheres are or will be soon (with JWST, EChO, Finesse, E-ELT) accessible to characterization. Cooler atmospheres will depart more from equilibrium and will thus be more sensitive to the details of the kinetics. Molecules that remain minor constituents of hot Jupiter atmospheres will become more abundant in cooler atmospheres and have an increased influence on their spectral appearance and thermal structure, making the use of validated schemes even more relevant. More metallic atmospheres should be found as we explore the exoplanet realm towards smaller objects with higher core/envelope masses, and eventually terrestrial objects. While some uncertainties still exist when applying our network to hydrogen-rich atmospheres, atmospheres with decreasing hydrogen to heavy elements ratio become closer to the conditions of validation (by their equivalence ratios, to use combustion terms). Even hot Jupiters can be significantly enriched (by factor of 10 or more) in heavy elements compared to their parent stars, which could for instance explain the high observed abundances of CO_2 (Zahnle et al. 2009a).

5. Conclusion

We have constructed a chemical scheme to study the atmospheric composition of hot Jupiters. Compared to existing models we chose to use one that
- is derived from mechanisms that are intensively used for industrial applications (in particular car engine simulations),
- has been subjected to in-depth validation protocols in a broad range of temperatures, pressures and compositions,
- is based on individual rate coefficient that have not been altered in order to optimize the agreement between the collective behavior of the network and experiments (contrary to most mechanisms in combustion). This allows users to apply the network slightly beyond its validation domain and to add species and reactions,
- uses experimental measurements for some of the endothermic reactions when robust data are available but still reproduces thermodynamic equilibrium with an excellent accuracy.

We developed a 1D photochemical model based on this kinetic scheme, and which includes vertical transport (mixing and molecular diffusion) and photodissociations. We applied this model to the hot Jupiters HD 209458b and HD 189733b and compared our results with those of Moses et al. (2011). Qualitatively, we find similar conclusions: photodissociations do not have a significant impact on the atmospheric composition of HD 209458b, with the high temperatures we assume. It remains at the thermodynamic equilibrium for pressures higher than 1 bar. For lower pressures vertical transport affects the abundances of HCN, NH_3 and CH_4 and some of the minor species associated. For HD 189733b, we assume significantly lower temperatures and find the atmospheric composition to be more sensitive to photolyses and vertical transport, all species being affected, except the main reservoirs, H_2, H_2O, CO and N_2. Quantitatively, however, we find significant differences (up to several orders of magnitude in the case of HD 189733b) in the abundances that are likely to be due to the different chemical schemes used. These differences are smaller for HD 209548b because kinetics have less influence. The quenching of HCN and NH_3, as well as CH_4 to a lower extent, is particularly affected, as well as most species sensitive to photochemistry in the upper atmosphere. Despite being large in terms of abundances, these differences do not pro-
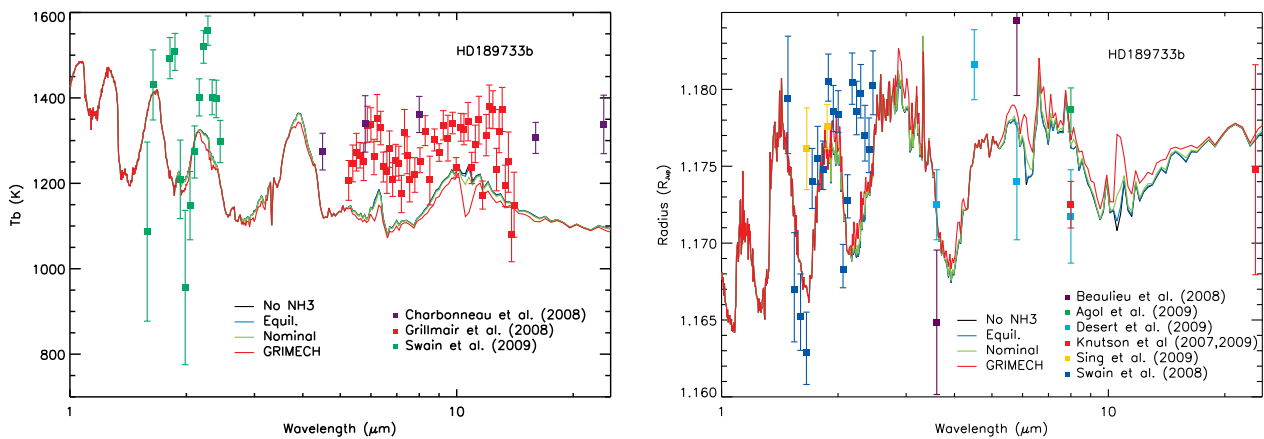
Fig. 10: Synthetic day-side (left) and transmission (right) spectra of HD 189733b with the nominal mechanism (green curve) compared to the one corresponding to the *GRIMECH* mechanism (red curve) and to the thermochemical equilibrium (blue curve). The dark curve is obtained when NH_3 is removed from the model. The day-side fluxes are given as brightness temperatures (T_b). Because of the reflection component, note that the link between T_b and the atmospheric thermal profile is altered below 2 μm. The transmission spectrum is given as the apparent planetary radius. The data points obtained from various observations are also shown.

duce strong effects on the spectra, with the exception of NH_3 at 10.5 μm. Confronting different schemes with observations will thus have to wait more accurate spectroscopic observations (JWST, E-ELT, EChO). Until that, experimental validation appears mandatory.

In order to illustrate the sensitivity to the kinetic scheme, we implemented different available nitrogen schemes, that are either optimized (*GRIMECH*, *GDFKin*) or non validated (*Dean*). We studied the extent of the possible results, and found large differences whenever disequilibrium chemistry is at work. Changing the nitrogen scheme strongly affects the quenched species (HCN, NH_3) and most species (including hydrocarbons) in the upper atmosphere of HD 189733b. For HD 209458b, deviations are again less noticeable as the atmosphere departs less from equilibrium. We therefore emphasize on the need to use validated and non optimized chemical schemes. This is already true for hot Jupiters but this is even more crucial in the case of cooler atmospheres (GJ1614b, GJ3470b, for instance), which depart more from thermodynamic equilibrium and are more sensitive to kinetics.

Our nominal scheme can be downloaded from the KIDA database[7] (Wakelam et al. 2012). The scheme is designed to reproduce the kinetic evolution of species with less than two carbon atoms. In order to study atmospheres with C/O ratio higher than solar (close to or above 1), we are currently developing a C_0-C_6 scheme, which will be able to describe kinetics of species up to 6 carbon atoms. One of the next improvement of our model should be the addition of sulfur. As kinetics of nitrogen species is an active field of research, we expect regular updates of the network (which would be notified and available on KIDA).

Note also that conclusions of this study on the chemical composition of hot Jupiters, which derive from models using an average 1D vertical profile, will probably have to be revisited with the effects of atmospheric circulation.

---

[7] http://kida.obs.u-bordeaux1.fr/

References

Agol, E., Cowan, N., Knutson, H., et al. 2010, The Astrophysical Journal, 721, 1861

Akimoto, H., Obi, K., & Tanaka, I. 1965, Journal of Chemical Physics, 42, 3864–3868

Allendorf, M. D. 2006, URL: http://www.ca.sandia.gov/HiTempThermo/index.hml

Anderlohr, J., Bounaceur, R., Pires Da Cruz, A., & Battin-Leclerc, F. 2009, Combustion and Flame, 156, 505

Anderlohr, J., Pires da Cruz, A., Bounaceur, R., & Battin-Leclerc, F. 2010, Combustion Science and Technology, 182, 39

Atakan, B. & Hartlieb, A. 2000, Applied Physics B: Lasers and Optics, 71, 697

Atkinson, R., Baulch, D., Cox, R., et al. 2006, Atmospheric Chemistry and Physics, 6, 3625

Atkinson, R., Baulch, D., Cox, R., et al. 1997, Journal of Physical and Chemical Reference Data, 26, 1329

Au, J., Cooper, G., Burton, G., Olney, T., & Brion, C. 1993, Chemical Physics, 173, 209

Balucani, N., Alagia, M., Cartechini, L., et al. 2000a, Journal of the American Chemical Society, 122, 4443

Balucani, N., Cartechini, L., Alagia, M., Casavecchia, P., & Volpi, G. 2000b, The Journal of Physical Chemistry A, 104, 5655

Barbé, P., Battin-Leclerc, F., & Côme, G. 1995, Journal de Chimie Physique, 92, 1666

Barman, T. 2007, ApJ, 661, L191

Batalha, N. M., Rowe, J. F., Bryson, S. T., et al. 2012, ArXiv e-prints

Battin-Leclerc, F., Blurock, E., Bounaceur, R., et al. 2011, Chemical Society Reviews, 40, 4762

Battin-Leclerc, F., Bounaceur, R., Belmekki, N., & Glaude, P. 2006, International Journal of Chemical Kinetics, 38, 284

Baulch, D., Bowman, C., Cobos, C., et al. 2005, Journal of Physical and Chemical Reference Data, 34, 757

Baulch, D., Cobos, C., Cox, R., et al. 1992, Journal of Physical and Chemical Reference Data, 21, 411

Baulch, D., Cobos, C., Cox, R., et al. 1994, Journal of Physical and Chemical Reference Data, 23, 847

Beaulieu, J., Carey, S., Ribas, I., & Tinetti, G. 2008, The Astrophysical Journal, 677, 1343

Beaulieu, J., Kipping, D., Batista, V., et al. 2010, Monthly Notices of the Royal Astronomical Society, 409, 963

Benson, S. W. 1976, Thermochemical Kinetics: methods for the estimation of thermochemical data and rate parameters, Second Edition (John Wiley, New York)

Benson, S. W. & Cohen, N. 1997, In Peroxyl Radicals (John Wiley, New York)

Bounaceur, R., Glaude, P., Fournet, R., et al. 2007, International Journal of Vehicle Design, 44, 124

Bounaceur, R., Herbinet, O., Fournet, R., et al. 2010, SAE Technical Paper, 01

Brown, M. J. & Smith, D. B. 1994, Symposium (International) on Combustion, 25, 1011 , 25th Symposium (International) on Combustion

Burrows, A., Budaj, J., & Hubeny, I. 2008, The Astrophysical Journal, 678, 1436

Burrows, A., Hubeny, I., Budaj, J., Knutson, H., & Charbonneau, D. 2007, The Astrophysical Journal Letters, 668, L171

Burrows, A. & Sharp, C. 1999, The Astrophysical Journal, 512, 843

Burton, G., Chan, W., Cooper, G., & Brion, C. 1993, Chemical Physics, 177, 217

Caridade, P., Rodrigues, S., Sousa, F., & Varandas, A. 2005, The Journal of Physical Chemistry A, 109, 2356

Cavalié, T., Billebaud, F., Biver, N., et al. 2008, Planetary and Space Science, 56, 1573

Cavalié, T., Billebaud, F., Dobrijevic, M., et al. 2009, Icarus, 203, 531

Chan, W., Cooper, G., & Brion, C. 1992, Chemical Physics, 168, 375

Chan, W., Cooper, G., & Brion, C. 1993a, Chemical Physics, 170, 111

Chan, W., Cooper, G., & Brion, C. 1993b, Chemical Physics, 178, 387

Chan, W., Cooper, G., Sodhi, R., & Brion, C. 1993c, Chemical Physics, 170, 81

Chang, A. H. H., Mebel, A. M., Yang, X.-M., Lin, S. H., & Lee, Y. T. 1998, The Journal of Chemical Physics, 109, 2748

Charbonneau, D., Brown, T., Latham, D., & Mayor, M. 2000, The Astrophysical Journal Letters, 529, L45

Charbonneau, D., Brown, T., Noyes, R., & Gilliland, R. 2002, The Astrophysical Journal, 568, 377

Charbonneau, D., Knutson, H., Barman, T., et al. 2008, The Astrophysical Journal, 686, 1341

Chen, F., Judge, D., Wu, C., & Caldwell, J. 1999, Planetary and Space Science, 47, 261–266

Chen, F. & Wu, C. 2004, Journal of Quantitative Spectroscopy and Radiative Transfer, 85, 195

Cheng, B., Lu, H., Chen, H., et al. 2006, The Astrophysical Journal, 647, 1535

Cody, R., Sabetydzvonik, M., & Jackson, W. 1977, Journal of Chemical Physics, 66, 2145–2152

Cooper, C. & Showman, A. 2006, The Astrophysical Journal, 649, 1048

Cooper, G., Anderson, J., & Brion, C. 1996, Chemical Physics, 209, 61

Cooper, G., Burton, G., & Brion, C. 1995a, Journal of Electron Spectroscopy and Related Phenomena, 73, 139

Cooper, G., Olney, T., & Brion, C. 1995b, Chemical Physics, 194, 175

Coppens, F., De Ruyck, J., & Konnov, A. 2007, Combustion and Flame, 149, 409

Dagaut, P., Glarborg, P., & Alzueta, M. 2008, Progress in Energy and Combustion Science, 34, 1

De Ferrieres, S., El Bakali, A., Lefort, B., Montero, M., & Pauwels, J. 2008, Combustion and Flame, 154, 601

Dean, A. & Bozzelli, J. 2000, Springer-Verlag Inc, 125

Désert, J., Lecavelier des Etangs, A., Hébrard, G., et al. 2009, The Astrophysical Journal, 699, 478

Dirrenberger, P., Le Gall, H., Bounaceur, R., et al. 2011, Energy & Fuels

Dobrijevic, M., Cavalié, T., Hébrard, E., et al. 2010, Planetary and Space Science, 1555

Dobrijevic, M., Hébrard, E., Plessis, S., et al. 2010, Adv. Space Res., 45, 77

Dobrijevic, M., Ollivier, J., Billebaud, F., Brillet, J., & Parisot, J. 2003, Astronomy and Astrophysics, 398, 335

Domalski, E. S. & Hearing, E. D. 1996, Journal of Physical and Chemical Reference Data, 25, 1

El Bakali, A., Pillier, L., Desgroux, P., et al. 2006, Fuel, 85, 896

Eng, R., Lambert, H., Fei, R., Carrington, T., & Filseth, S. 1996, Chemical Physics Letters, 261, 651

Eriksson, G. & Rosen, E. 1971, Acta Polytechnica Scandinavica - Chemical Including Metallurgy Series, 2-32

Fahr, A., Hassanzadeh, P., & Atkinson, D. 1998, Chemical Physics, 236, 43

Fillion, J., Ruiz, J., Yang, X., et al. 2004, The Journal of Chemical Physics, 120, 6531

Fortney, J., Cooper, C., Showman, A., Marley, M., & Freedman, R. 2006, The Astrophysical Journal, 652, 746

Fortney, J., Lodders, K., Marley, M., & Freedman, R. 2008a, The Astrophysical Journal, 678, 1419

Fortney, J., Marley, M., Saumon, D., & Lodders, K. 2008b, The Astrophysical Journal, 683, 1104

Fournet, R., Baugé, J., & Battin-Leclerc, F. 1999, International Journal of Chemical Kinetics, 31, 361

Gans, B., Boye-Peronne, S., Broquier, M., et al. 2011, Physical Chemistry Chemical Physics, 13, 8140

Gardner, J. P., Mather, J. C., Clampin, M., et al. 2006, Space Science Reviews, 123, 485

Gibbs, J. 1873, A method of geometrical representation of the thermodynamic properties of substances by means of surfaces (Connecticut Academy of Arts and Sciences)

Gladstone, G., Allen, M., & Yung, Y. 1996, Icarus, 119, 1

Glaude, P., Marinov, N., Koshiishi, Y., Matsunaga, N., & Hori, M. 2005, Energy & Fuels, 19, 1839

Golden, D. 2008, International Journal of Chemical Kinetics, 40, 310

Goose, E., Burcat, A., & Ruscic, R. 2010, URL: http://garfield.chem.elte.hu/Burcat/burcat.html4

Grenfell, J., Lehmann, R., Mieth, P., Langematz, U., & Steil, B. 2006, Journal of geophysical research, 111, D17311

Grillmair, C., Burrows, A., Charbonneau, D., et al. 2008, Nature, 456, 767

Hampson Jr, R. & McNesby, J. 1965, The Journal of Chemical Physics, 42, 2200

Hauschildt, P., Allard, F., & Baron, E. 1999, The Astrophysical Journal, 512, 377

Hébrard, E., Dobrijevic, M., Bénilan, Y., & Raulin, F. 2006, Journal of Photochemistry and Photobiology C: Photochemistry Reviews, 7, 211

Hébrard, E., Dobrijevic, M., Bénilan, Y., & Raulin, F. 2007, Planetary and Space Science, 55, 1470

Herron, J. 1999, Journal of Physical and Chemical Reference Data, 28, 1453

Hochanadel, C., Sworski, T., & Ogren, P. 1980, The Journal of Physical Chemistry, 84, 231

Holland, D., Shaw, D., Hayes, M., et al. 1997, Chemical Physics, 219, 91

Howard, A., Marcy, G., Johnson, J., et al. 2010, Science, 330, 653

Howard, A., Marcy, G. W., Bryson, S. T., et al. 2012, The Astrophysical Journal Supplement Series, 201, 15

Huebner, W., Keady, J., & Lyon, S. 1992, Solar photo rates for planetary atmospheres and atmospheric pollutants (Kluwer Academic Pub)

Huestis, D. L. & Berkowitz, J. 2010, Advances in Geosciences, 25, 229

Huffman, R. 1969, Canadian Journal of Chemistry, 47, 1823

Huitson, C. M., Sing, D. K., Vidal-Madjar, A., et al. 2012, ArXiv e-prints

Iida, Y., Carnovale, F., Daviel, S., & Brion, C. 1986, Chemical Physics, 105, 211

Iro, N., Bézard, B., & Guillot, T. 2005, Astronomy and Astrophysics, 436, 719

Iro, N. & Deming, L. D. 2010, The Astrophysical Journal, 712, 218

Isaksen, I. S. A., Midtbo, K. H., Sunde, J., & Crutzen, P. J. 1977, Geophysica Norvegica, 31, 11

Ityakov, D., Linnartz, H., & Ubachs, W. 2008, Chemical Physics Letters, 462, 31

Jackson, W. & Halpern, J. 1979, The Journal of Chemical Physics, 70, 2373

Kameta, K., Kouchi, N., Ukai, M., & Hatano, Y. 2002, Journal of Electron Spectroscopy and Related Phenomena, 123, 225

Kameta, K., Machida, S., Kitajima, M., et al. 1996, Journal of Electron Spectroscopy and Related Phenomena, 79, 391 , proceedings of the 11th International Conference on Vacuum Ultraviolet Radiation Physics

Khamaganov, V., Karunanandan, R., Rodriguez, A., & Crowley, J. 2007, Physical Chemistry Chemical Physics, 9, 4098

Knutson, H., Charbonneau, D., Cowan, N., et al. 2009, The Astrophysical Journal, 690, 822

Knutson, H. A., Charbonneau, D., Allen, L. E., et al. 2007, Nature, 447, 183

Ko, T., Marshall, P., & Fontijn, A. 1990, Journal of Physical Chemistry, 94, 1401

Konnov, A. A. 2000, in 28-th Symposium (Int.) on Combustion. Abstr. Symp. Pap, 317

Konnov, A. A. 2009, Combustion and Flame, 156, 2093

Konnov, A. A. & De Ruyck, J. 1999a, Combustion Science and Technology, 149, 53

Konnov, A. A. & De Ruyck, J. 1999b, in Mediterranean Combustion Symposium, 679–690

Konnov, A. A. & De Ruyck, J. 2000a, in 16th International Symposium on Gas Kinetics, Cambridge, Abstr. Symp. Pap. PC10

Konnov, A. A. & De Ruyck, J. 2000b, Combustion Science and Technology, 152, 23

Konnov, A. A. & De Ruyck, J. 2001a, Combustion and Flame, 125, 1249

Konnov, A. A. & De Ruyck, J. 2001b, Combustion and Flame, 124, 106

Lamoureux, N., Desgroux, P., El Bakali, A., & Pauwels, J. 2010, Combustion and Flame, 157, 1929

Langland-Shula, L., Vogt, S., Charbonneau, D., Butler, P., & Marcy, G. 2009, The Astrophysical Journal, 696, 1355

Lee, A., Yung, Y., Cheng, B., et al. 2001, The Astrophysical Journal Letters, 551, L93

Lee, L. 1980, The Journal of Chemical Physics, 72, 6414

Lehmann, R. 2004, Journal of atmospheric chemistry, 47, 45

Liang, M., Parkinson, C., Lee, A., Yung, Y., & Seager, S. 2003, The Astrophysical Journal Letters, 596, L247

Liang, M., Seager, S., Parkinson, C., Lee, A., & Yung, Y. 2004, The Astrophysical Journal Letters, 605, L61

Lias, S. G., Collin, G. J., Rebbert, R. E., & Ausloos, P. 1970, The Journal of Chemical Physics, 52, 1841

Lindemann, F., Arrhenius, S., Langmuir, I., et al. 1922, Transactions of the Faraday Society, 17, 598

Line, M., Liang, M., & Yung, Y. 2010, The Astrophysical Journal, 717, 496

Lodders, K. & Fegley, B. 2002, Icarus, 155, 393

Lodders, K. & Palme, H. 2009, Meteoritics and Planetary Science Supplement, 72, 5154

Loison, J.-C., Kable, S. H., Houston, P. L., & Burak, I. 1991, Journal of Chemical Physics, 94, 1796

Luo, Y. 2003, Handbook of bond dissociation energies in organic compounds (CRC)

Madhusudhan, N., Harrington, J., Stevenson, K., et al. 2011a, Nature, 469, 64

Madhusudhan, N., Mousis, O., Johnson, T., & Lunine, J. 2011b, The Astrophysical Journal, 743, 191

Madhusudhan, N. & Seager, S. 2009, The Astrophysical Journal, 707, 24

Madhusudhan, N. & Seager, S. 2010, The Astrophysical Journal, 725, 261

Manion, J. A., Huie, R. E., Levin, R. D., et al. 2008, NIST Chemical Kinetics Database, NIST Standard Reference Database 17

McBride, B., Gordon, S., & Reno, M. 1993, NASA Technical Memorandum, 4513

McNesby, J., Tanaka, I., & Okabe, H. 1962, The Journal of Chemical Physics, 36, 605

Mebel, A. M., Lin, M. C., & Morokuma, K. 1998, International Journal of Chemical Kinetics, 30

Meller, R. & Moortgat, G. 2000, Journal of Geophysical Research, 105, 7089

Merienne, M., Jenouvrier, A., Coquart, B., & Lux, J. 1997, Journal of Atmospheric Chemistry, 27, 219

Michael, J., Sutherland, J., & Klemm, R. 1986, The Journal of Physical Chemistry, 90, 497

Moses, J., Allen, M., & Gladstone, G. 1995a, Geophysical Research Letters, 22, 1601

Moses, J., Allen, M., & Gladstone, G. 1995b, Geophysical Research Letters, 22, 1597

Moses, J., Bézard, B., Lellouch, E., et al. 2000a, Icarus, 143, 244

Moses, J., Lellouch, E., Bézard, B., et al. 2000b, Icarus, 145, 166

Moses, J., Visscher, C., Fortney, J., et al. 2011, The Astrophysical Journal, 737, 15

Moses, J. I. 1996, in The Collision of Comet Shoemaker-Levy 9 and Jupiter (ed. H. A. Weaver, K. S. Noll, P. D. Feldman (Cambridge, UK: Cambridge Univ. Press))

Mota, R., Parafita, R., Giuliani, A., et al. 2005, Chemical Physics Letters, 416, 152

Mount, G. & Moos, H. 1978, The Astrophysical Journal, 224, L35

Muller, C., Michel, V., Scacchi, G., & Côme, G. 1995, Journal de Chimie Physique, 92, 1154

Okabe, H. 1978, Photochemistry of small molecules (Wiley New York)

Okabe, H. 1981, The Journal of Chemical Physics, 75, 2772

Okabe, H. 1983, The Journal of Chemical Physics, 78, 1312

Olney, T., Cann, N., Cooper, G., & Brion, C. 1997, Chemical Physics, 223, 59

Orkin, V., Huie, R., & Kurylo, M. 1997, The Journal of Physical Chemistry A, 101, 9118

Parkes, D., Paul, D., Quinn, C., & Robson, R. 1973, Chemical Physics Letters, 23, 425

Reynolds, W. C. 1986, Technical Report

Richardson, L., Deming, D., Horning, K., Seager, S., & Harrington, J. 2007, Nature, 445, 892

Rothman, L. S., Gordon, I. E., Barbe, A., et al. 2009, Journal of Quantitative Spectroscopy and Radiative Transfer, 110, 533

Rowe, J., Matthews, J., Seager, S., et al. 2008, The Astrophysical Journal, 689, 1345

Samson, J. & Cairns, R. 1964, Journal of Geophysical Research, 69, 4583

Samson, J. & Haddad, G. 1994, JOSA B, 11, 277

Sander, S. P., Friedl, R. R., Barker, J. R., et al. 2011, NASA/JPL Publication

Sanz-Forcada, J., Micela, G., Ribas, I., et al. 2011, Astronomy and Astrophysics, 532, A6

Sato, K., Misawa, K., Kobayashi, Y., et al. 1999, The Journal of Physical Chemistry A, 103, 8650

Schultz, E. & Shepherd, J. 1999, California Institute of Technology, Graduate Aeronautical Laboratories, Technical Report FM99-5

Seager, S. & Sasselov, D. 2000, The Astrophysical Journal, 537, 916

Selsis, F., Despois, D., & Parisot, J. 2002, Astronomy and Astrophysics, 388, 985

Sharp, C. & Burrows, A. 2007, The Astrophysical Journal Supplement Series, 168, 140

Showman, A., Fortney, J., Lian, Y., et al. 2009, The Astrophysical Journal, 699, 564

Sing, D., Désert, J., des Etangs, A., et al. 2009, Astronomy and Astrophysics, 505, 891

Sing, D., Vidal-Madjar, A., Désert, J., Etangs, A., & Ballester, G. 2008, The Astrophysical Journal, 686, 658

Smith, G., Golden, D., Frenklach, M., et al. 1999, URL: http://www. me. berkeley. edu/gri_mech

Smith, W. & Missen, R. 1982, Chemical reaction equilibrium analysis: theory and algorithms (Wiley New York)

Southworth, J. 2008, Monthly Notices of the Royal Astronomical Society, 386, 1644

Southworth, J. 2010, Monthly Notices of the Royal Astronomical Society

Stark, G., Smith, P. L., Huber, K. P., et al. 1992, Journal of Chemical Physics, 97, 4809–4814

Stark, G., Yoshino, K., Smith, P. L., & Ito, K. 2007, Journal of Quantitative Spectroscopy & Radiative Transfer, 103, 67

Stewart, P., Larson, C., & Golden, D. 1989, Combustion and Flame, 75, 25

Stock, J., Boxe, C., Lehmann, R., et al. 2012, Icarus, 219, 13

Stock, J., Grenfell, J., Lehmann, R., Patzer, A., & Rauer, H. 2011, Planetary and Space Science

Stockwell, W. & Calvert, J. 1978, Journal of Photochemistry, 8, 193

Swain, M., Bouwman, J., Akeson, R., Lawler, S., & Beichman, C. 2008a, The Astrophysical Journal, 674, 482

Swain, M., Tinetti, G., Vasisht, G., et al. 2009a, The Astrophysical Journal, 704, 1616

Swain, M., Vasisht, G., & Tinetti, G. 2008b, Nature, 452, 329

Swain, M., Vasisht, G., Tinetti, G., et al. 2009b, The Astrophysical Journal Letters, 690, L114

Swain, M. R. 2010, in Bulletin of the American Astronomical Society, Vol. 42, AAS/Division for Planetary Sciences Meeting Abstracts #42, 1064

Thielen, K. & Roth, P. 1986, AIAA journal, 24, 1102

Tinetti, G., Beaulieu, J. P., Henning, T., et al. 2011, ArXiv e-prints

Tinetti, G., Vidal-Madjar, A., Liang, M., et al. 2007, Nature, 448, 169

Troe, J. 1983, Berichte der Bunsengesellschaft für Physikalische Chemie, 87, 161

Troe, J. 2011, Combustion and Flame, 158, 594

Tsang, W. 1987, Journal of Physical and Chemical Reference Data, 16, 471

Tsang, W. 1991, Journal of Physical and Chemical Reference Data, 20, 221

Tsang, W. & Hampson, R. 1986, Journal of Physical and Chemical Reference Data, 15, 1087

Tsang, W. & Herron, J. 1991, Journal of Physical and Chemical Reference Data, 20, 609

Turbiez, A., Pauwels, J., Desgroux, P., et al. 1998, in 27th Symposium (international) on Combustion

Umemoto, H., Nakae, T., Hashimoto, H., & Kongo, K. 1998, Journal of Chemical Physics, 109, 5844

Vaghjiani, G. 1995, International Journal of Chemical Kinetics, 27, 777

Vaghjiani, G. L. 1993, Journal of Chemical Physics, 98, 2123

Van Dishoeck, E. & Dalgarno, A. 1984, Icarus, 59, 305

Vandaele, A., Hermans, C., Simon, P., et al. 1998, Journal of Quantitative Spectroscopy and Radiative Transfer, 59, 171

Visscher, C., Lodders, K., & Fegley, Jr., B. 2006, The Astrophysical Journal, 648, 1181

Visscher, C., Lodders, K., & Fegley, Jr., B. 2010, The Astrophysical Journal, 716, 1060

Wakelam, V., Herbst, E., Loison, J.-C., et al. 2012, The Astrophysical Journal Supplement Series, 199, 21

Wang, H., Warner, S., Oehlschlaeger, M., et al. 2010, Combustion and Flame, 157, 1976

White, W., Johnson, S., & Dantzig, G. 1958, The Journal of Chemical Physics, 28, 751

Wu, C., Chen, F., & Judge, D. 2001, Journal of Geophysical Research, 106, 7629

Wu, C., Chen, F., & Judge, D. 2004, Journal of Geophysical Research, 109, E07S15

Zahnle, K., Marley, M., Freedman, R., Lodders, K., & Fortney, J. 2009a, The Astrophysical Journal Letters, 701, L20

Zahnle, K., Marley, M. S., & Fortney, J. J. 2009b, eprint arXiv:0911.0728

Appendix A: Thermochemical data

Thermochemical properties, such as enthalpies of formation, entropies and heat capacities are of great importance to ensure the consistency between the rate parameters of the forward and reverse elementary reactions. They are also useful to estimate the heat release rate. Thermochemical data for all molecules or radicals have been estimated and stored as 14 NASA polynomial coefficients, according to the McBride et al. (1993) formalism. The NASA polynomials have the following form:

$$\frac{c_p^0(T)}{RT} = a_1 + a_2 T + a_3 T^2 + a_4 T^3 + a_5 T^4 \tag{A.1}$$

$$\frac{h^0(T)}{RT} = a_1 + a_2 \frac{T}{2} + a_3 \frac{T^2}{3} + a_4 \frac{T^3}{4} + a_5 \frac{T^4}{5} + \frac{a_6}{T} \tag{A.2}$$

$$\frac{s^0(T)}{R} = a_1 \ln T + a_2 T + a_3 \frac{T^2}{2} + a_4 \frac{T^3}{3} + a_5 \frac{T^4}{4} + a_7 \tag{A.3}$$

Where a_i, $i \in [1, 7]$, are the numerical NASA coefficients for the fourth-order polynomial. Each species is characterized by fourteen numbers. The first seven numbers are for the high-temperature range, generally from 1000 to 5000 K, and the following seven numbers are the coefficients for the low-temperature range, generally from 300 to 1000 K. When these parameters are not available in the literature (McBride et al. 1993; Allendorf 2006; Goose et al. 2010) which is the most frequent case for species present in automotive fuels, they have to be estimated. In this case, these data were automatically calculated using the software THERGAS (Muller et al. 1995), developed in the LRGP laboratory, based on the group and bond additivity methods proposed by Benson (1976) and updated based on the data of Domalski & Hearing (1996). The enthalpies of formation of alkyl radicals have been also updated according to the values of bond dissociation energies published by Tsang & Hampson (1986) and by Luo (2003) and following the recommendations of Benson & Cohen (1997) respectively.

An elementary reversible reaction i involving L chemical species can be represented in the following general form:

$$\sum_{l=1}^{L} \nu'_{li} \chi_l \Leftrightarrow \sum_{l=1}^{L} \nu''_{li} \chi_l \tag{A.4}$$
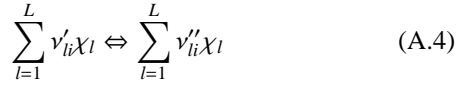
where ν'_{li} are the forward stoichiometric coefficients, and ν''_{li} are the reverse ones. χ_l is the chemical symbol of the lth species.

The kinetic data associated to each reaction are expressed with a modified Arrhenius law $k(T) = A \times T^n \exp^{-\frac{E_a}{RT}}$ where T is the temperature, E_a is the activation energy of the reaction, A the pre-exponential factor and n a coefficient which allows the temperature dependence of the pre-exponential factor. If the rate constant associated to the forward reaction is $k_{fi}(T)$, then the one associated to the reverse reaction is $k_{ri}(T)$, verifying:

$$K_{pi} = \frac{k_{fi}(T)}{k_{ri}(T)} \left(\frac{k_B T}{P^0} \right)^{\sum_{l=1}^{L} \nu_{li}} \tag{A.5}$$

where K_{pi} is the equilibrium constant, when the activity of the reactants is expressed in pressure units (Benson 1976):

$$K_{pi} = \exp \left(\frac{\Delta S_i^0}{R} - \frac{\Delta H_i^0}{RT} \right) \tag{A.6}$$

where ΔS_i^0 and ΔH_i^0 are the variation of entropy and enthalpy occurring when passing from reactants to products in the reaction i, P^0 is the standard pressure ($P^0 =$1,01325 bar), k_B is the Boltzmann's constant and ν_l are the stoichiometric coefficients of the L species involved in reaction i: $\nu_l = \nu''_{li} - \nu'_{li}$. Combined with Eqs. (A.2) and (A.3), $\frac{\Delta S_i^0}{R}$ and $\frac{\Delta H_i^0}{RT}$ can be calculated with the NASA coefficients:

$$\frac{\Delta S_i^0}{R} = \sum_{l=1}^{L} \nu_l \frac{s_l^0(T)}{R} \quad \text{and} \quad \frac{\Delta H_i^0}{RT} = \sum_{l=1}^{L} \nu_l \frac{h_l^0(T)}{RT} \tag{A.7}$$

Finally, we can calculate the reverse reaction rate for the reaction i:

$$k_{ri}(T) = \frac{k_{fi}(T)}{K_{pi}} \left(\frac{k_B T}{P^0} \right)^{\sum_{l=1}^{L} \nu_{li}} \tag{A.8}$$

Appendix B: Chemical equilibrium calculation

To compute the equilibrium abundance of the species in a definite system considered as an ideal gas, we have developed a Thermodynamical Equilibrium Calculator TECA. TECA is a software which allows the equilibrium calculation for a complex mixture. More specifically, for a given initial state of an ideal-gas mixture, the chemical-equilibrium program is able to determine the gas composition at a defined temperature and pressure. This calculation is based on the principle of the minimization of Gibbs energy (e.g. Gibbs 1873; White et al. 1958; Eriksson & Rosen 1971; Smith & Missen 1982; Reynolds 1986):

$$G = \sum_{l=1}^{L} \overline{g_l} N_l \tag{B.1}$$

where L is the total number of species, $\overline{g_l}$ is the partial free energy of the species l and N_l is the number of moles of the species l.

The partial free energy of a compound l, behaving as an ideal gas, is given by:

$$\overline{g_l} = g_l(T, P) + RT \ln N_l \tag{B.2}$$

where $g_l(T, P)$ is the free energy of the species l at the temperature T and the pressure P of the system and R is the ideal gas constant.

For an ideal gas, $g_l(T, P)$ is given by:

$$g_l(T, P) = h_l^0(T) - T s_l^0(T) + RT \ln \left(\frac{P}{P^0} \right) \tag{B.3}$$

where $h_l^0(T)$ and $s_l^0(T)$ are respectively, the standard-state enthalpy and entropy of the species l at the temperature T of the system.

The enthalpy and the entropy are expressed as NASA polynomials as described above.

Appendix C: Pressure-dependent reactions

Under some conditions, several reactions do not have the same rate constant depending if they occur under low or high pressure (respectively $k_0(T)$ and $k_\infty(T)$). In this case, between these two limits it appears what is called a fall-off zone. This is typically the case in reactions requiring a collisional body to proceed, such as thermal dissociation or recombination (three-body) reactions. In the present kinetic model we have different types of reactions with pressure dependent rate constants (Table C.1). In some cases, some species act more efficiently as collisional bodies than do others. Then, when available from literature, collisional efficiencies are used to specify the increased efficiency of the lth species in the ith reaction (see for example reaction (2) in Table C.1).

For the pressure-dependent reactions, the rate constant at any pressure is taken to be:

$$k(T) = k_\infty(T) \left(\frac{P_r}{1 + P_r} \right) F \tag{C.1}$$

where the reduced pressure P_r is given by:

$$P_r = \frac{[M] k_0}{k_\infty} \tag{C.2}$$

and $[M]$ is the concentration of the mixture, weighted by the efficiency of each compound, α_l, in the reaction studied:

$$[M] = \sum_{l=1}^{L} \alpha_l [X_l] \qquad (C.3)$$

where $[X_l]$ is the concentration of the species k.

As shown in Table C.1, three methods of representation of the rate expression in the fall-off region are used (enhanced collisional body efficiencies of certain species are presented below the reaction):

- the Lindemann et al. (1922) formulation, illustrated by reaction (1) in Table C.1;
- the Troe (1983) formulation, see for example reaction (2) in Table C.1;
- the SRI formulation proposed by Stewart et al. (1989), illustrated by reaction (3) in Table C.1.

In the Lindenman form, F is unity ($F=1$).
In the Troe form F is given by

$$\log_{10} F = \frac{\log_{10}(F_{cent})}{1 + \left[\frac{\log_{10}(P_r)+c}{N-d(\log_{10}(P_r)+c)}\right]^2} \qquad (C.4)$$

with

$$c = -0.4 - 0.67 \times \log_{10}(F_{cent})$$
$$N = 0.75 - 1.27 \times \log_{10}(F_{cent})$$
$$d = 0.14$$

and

$$F_{cent} = (1-a)\exp\left(-\frac{T}{T^{***}}\right) + a\exp\left(-\frac{T}{T^*}\right) + \exp\left(-\frac{T^{**}}{T}\right) \quad (C.5)$$

The four parameters a, T^{***}, T^* and T^{**} must be specified but it is often the case that the parameter T^{**} is not used by lack of data.

The approach taken at the Stanford Research Institute (SRI) by Stewart et al. (1989) is in many ways similar to that taken by Troe, but the blending function F is approximated differently. Here, F is given by

$$F = d\left[a\exp\frac{-b}{T} + \exp\frac{-T}{c}\right]^X T^e \qquad (C.6)$$

where

$$X = \frac{1}{1 + (\log_{10} P_r)^2} \qquad (C.7)$$

Appendix D: Photodissociations

	Reaction considered				$k = AT^n \exp(-E/RT)$ A (cm^3.molecule^{-1}.s^{-1}.K^{-n})	$-$ High pressure limit n	E/R (K)
1.	C2H4+OH(+M)=C2H4OH(+M)				9.003×10^{-12}	0.0	0.0
	Low pressure limit:	3.284×10^{-21}	-3.1		0.0		
2.	H+CH3(+M)=CH4(+M)				2.774×10^{-10}	0.0	0.0
	O2	Enhanced by	0.40				
	CO	Enhanced by	0.75				
	CO2	Enhanced by	1.50				
	H2O	Enhanced by	6.50				
	CH4	Enhanced by	0.00^8				
	C2H6	Enhanced by	3.00				
	Ar	Enhanced by	0.35				
	N2	Enhanced by	0.40				
	He	Enhanced by	0.35				
	Low pressure limit:	3.885×10^{-24}	-1.8		0.0		
	TROE centering	0.37	3315		61		
3.	NO+OH(+M)=HONO(+M)				1.827×10^{-10}	-0.3	0.0
	Low pressure limit:	6.484×10^{-25}	-2.4		0.0		
	SRI centering:	1.0	0.0		1.00×10^{-18}	0.81	0.0

Table C.1: Some example of reactions with pressure-dependent rate constants present in the kinetic model.

Pathways			Cross sections	Quantum yields
J1	$H_2O + h\nu$	$\longrightarrow H + OH$	Chan et al. (1993b) and	Huebner et al. (1992)
J2		$\longrightarrow H_2 + O(^1D)$	Fillion et al. (2004) and	
J3		$\longrightarrow H + H + O(^3P)$	Mota et al. (2005)	
J4	$CO_2 + h\nu$	$\longrightarrow CO + O(^3P)$	Stark et al. (2007); Ityakov et al. (2008), and	Huebner et al. (1992)
J5		$\longrightarrow CO + O(^1D)$	Huestis & Berkowitz (2010)	
J6	$H_2CO + h\nu$	$\longrightarrow H_2 + CO$	Cooper et al. (1996)	Huebner et al. (1992)
J7		$\longrightarrow H + HCO$	and Meller & Moortgat (2000)	
J8	$OH + h\nu$	$\longrightarrow H + O(^1D)$	Huebner et al. (1992)	Van Dishoeck & Dalgarno (1984)
J9	$CO + h\nu$	$\longrightarrow C + O(^3P)$	Olney et al. (1997)	Huebner et al. (1992)
J10	$H_2 + h\nu$	$\longrightarrow H + H$	Samson & Haddad (1994); Chan et al. (1992)	Estimation
			Olney et al. (1997)	
J11	$CH_4 + h\nu$	$\longrightarrow CH_3 + H$	Au et al. (1993) and	Gans et al. (2011)
J12		$\longrightarrow {}^1CH_2 + H_2$	Lee et al. (2001) and	
J13		$\longrightarrow {}^3CH_2 + H + H$	Kameta et al. (2002) and	
J14		$\longrightarrow CH + H_2 + H$	Chen & Wu (2004)	
J15	$CH_3 + h\nu$	$\longrightarrow {}^1CH_2 + H$	Khamaganov et al. (2007)	Parkes et al. (1973)
J16	$C_2H_2 + h\nu$	$\longrightarrow C_2H + H$	Cooper et al. (1995a); Wu et al. (2001)	Okabe (1981, 1983)
J17	$C_2H_3 + h\nu$	$\longrightarrow C_2H_2 + H$	Fahr et al. (1998)	Fahr et al. (1998)
J18	$C_2H_4 + h\nu$	$\longrightarrow C_2H_2 + H_2$	Cooper et al. (1995b)	Holland et al. (1997)
J19		$\longrightarrow C_2H_2 + H + H$	Orkin et al. (1997) and Wu et al. (2004)	Chang et al. (1998)
J20	$C_2H_6 + h\nu$	$\longrightarrow C_2H_4 + H_2$	Au et al. (1993); Kameta et al. (1996)	Akimoto et al. (1965)
J21		$\longrightarrow C_2H_4 + H + H$	Lee et al. (2001)	Hampson Jr & McNesby (1965)
J22		$\longrightarrow C_2H_2 + H_2 + H_2$	Chen & Wu (2004)	Lias et al. (1970)
J23		$\longrightarrow CH_4 + {}^1CH_2$		Mount & Moos (1978)
J24		$\longrightarrow CH_3 + CH_3$		Mount & Moos (1978)
J25	$N_2 + h\nu$	$\longrightarrow N(^2D) + N(^4S)$	Samson & Cairns (1964); Huffman (1969)	Estimation
			Stark et al. (1992); Chan et al. (1993c)	
J26	$HCN + h\nu$	$\longrightarrow CN + H$	Lee (1980)	Lee (1980)
J27	$NH_3 + h\nu$	$\longrightarrow NH_2 + H$	Burton et al. (1993); Chen et al. (1999); Cheng et al. (2006)	McNesby et al. (1962)
J28	$NO + h\nu$	$\longrightarrow N(^4S) + O(^3P)$	Iida et al. (1986); Chan et al. (1993a)	Huebner et al. (1992)
J29	$N_2H_4 + h\nu$	$\longrightarrow N_2H_3 + H$	Vaghjiani (1993)	Vaghjiani (1993, 1995)
J30	$HNO_3 + h\nu$	$\longrightarrow NO_2 + OH$	Sander et al. (2011)	Estimation
J31	$C_2N_2 + h\nu$	$\longrightarrow CN + CN$	Bénilan et al. (2012), in preparation	Cody et al. (1977); Jackson & Halpern (1979); Eng et al. (1996)
J32	$N_2O_4 + h\nu$	$\longrightarrow NO_2 + NO_2$	Vandaele et al. (1998); Merienne et al. (1997)	Sander et al. (2011)
J33	$N_2O_3 + h\nu$	$\longrightarrow NO_2 + NO$	Stockwell & Calvert (1978)	Sander et al. (2011)
J34	$HCO + h\nu$	$\longrightarrow H + CO$	Hochanadel et al. (1980); Loison et al. (1991)	Estimation

Table D.1: Photodissociations scheme used in the model